Fall 2010

Arsenic speciation in the presence of anoxic mixed valent iron systems

Angela Meagan Brown
University of Iowa

ARSENIC SPECIATION IN THE PRESENCE OF ANOXIC MIXED VALENT IRON SYSTEMS

by

Angela Meagan Brown

A thesis submitted in partial fulfillment of the requirements for the
Master of Science degree in Civil and Environmental Engineering
in the Graduate College of
The University of Iowa

December 2010

Thesis Supervisor: Professor Michelle M. Scherer

Graduate College
The University of Iowa
Iowa City, Iowa

CERTIFICATE OF APPROVAL

_____

MASTER'S THESIS

_____

This is to certify that the Master's thesis of

Angela Meagan Brown

has been approved by the Examining Committee for the thesis requirement for the Master of Science degree in Civil and Environmental Engineering at the December 2010 graduation.

Thesis Committee: _____
Michelle M. Scherer, Thesis Supervisor

_____
Richard L. Valentine

_____
Gene F. Parkin

To my parents for nurturing my creative and academic pursuits

Success is the sum of small efforts, repeated day in and day out.

Robert Collier, Author of *The Secret of the Ages*

ACKNOWLEDGMENTS

I would like to thank Jay Thompson and David Peate for their generosity with the ICP-MS. Jay played a crucial role in developing the arsenic analytical method, and always provided me with a tuned and sensitive instrument for sample analysis.

I would also like to thank Ed O'Loughlin, Max Boyanov, and Argonne National Laboratory for their willingness to provide XAS data for my project.

My advisor, Michelle Scherer, has taught me a great deal about aquatic geochemistry and the scientific method through the opportunity she provided me to research in the laboratory. She has also provided invaluable guidance in solving problems, maintaining focus, and making sense of data. If anyone is capable of gleaning information out of this thesis, it is due to her ability to present information in an approachable manner.

The research assistants in Michelle's group helped me through countless struggles. I doubt I would even know how to pipette correctly without their guidance. I would like to thank Rob Handler, especially, for providing me with the basic knowledge and tools to pursue scientific inquiries. He was always willing to help, even in the midst of writing his own dissertation.

Lastly, I thank my friends and family for helping me keep things in perspective and providing love and support. The journey hasn't always been easy, but it has been very rewarding.

This research was generously funded by CGRER at The University of Iowa.

ABSTRACT

Iron is ubiquitous in the environment, ranking fourth in abundance in the earth's crust. Iron is responsible for many environmental mechanisms including the distribution of plant nutrients and pollutants. Iron can exist in several minerals, including iron oxides. Arsenic is a naturally occurring metalloid which has been confirmed by the EPA as a carcinogen. Recently, an arsenic epidemic has developed in Bangladesh, poisoning an estimated 70 million people. Arsenic contamination does not exist only in the third world, but also in the United States, including Iowa. Due to the widespread distribution of arsenic and the potential for it to be leached into groundwater supplies, there has been a growing interest in establishing removal mechanisms.

Atomic absorption (AA) spectroscopy and inductively coupled plasma optical emission spectrometry (ICP-OES) have been the traditional methods to measure arsenic. There has been a shift in arsenic analysis methods with the advent of more sensitive methods such as the inductively coupled plasma mass spectrometer (ICP-MS). We recently acquired a Thermo Scientific XSERIES ICP-MS at The University of Iowa, which we used to develop an arsenic analysis method in preparation for the research conducted in this study. The ICP-MS, however, only measures total arsenic concentration. As this study focused on the redox chemistry of arsenic, an alternative means for determining oxidation state was developed. As(V)-selective cartridges were used to adsorb arsenate (AsO_4^{3-}), while letting arsenite (AsO_3^{3-}) run through. This method was checked for effectiveness and used to determine aqueous arsenic oxidation state. X-ray absorption spectroscopy (XAS) was used to determine the oxidation state of arsenic adsorbed onto the surface of the iron oxide.

Goethite (α-FeOOH) and magnetite (Fe_3O_4) are both known to strongly adsorb arsenic. In this work, the potential for As(III) oxidation and As(V) reduction by goethite was studied. As documented by Amstaetter *et al*. (2010), there was some evidence for adsorbed As(III) oxidation by an Fe(II)/goethite system. This study, however, also showed some evidence for oxidation of adsorbed arsenite in the presence of goethite alone. As(V) reduction by magnetite was also studied. Magnetite is capable of having different stoichiometries, or ratios of Fe(II) to Fe(III). Both an oxidized, $x = 0.27$, and a near-stoichiometric, $x = 0.49$, magnetite were studied for their ability to reduce arsenate. There was no evidence for As(V) reduction in the aqueous or adsorbed phase for either system.

TABLE OF CONTENTS

LIST OF TABLES

LIST OF FIGURES

CHAPTER I INTRODUCTION

Iron in the Environment

Iron is the fourth most abundant element in the earth's crust. Much of the iron in the environment is present in iron oxides which can be found in soils, rocks, freshwater, the atmosphere, the ocean floor, and organisms. In soils, iron oxides have been shown to regulate the concentration and distribution of plant nutrients (Reynolds and Davies, 2001) and some pollutants. In biota, iron can be an essential element. Vertebrates rely on iron-containing hemoglobin to transport oxygen through the body. Many animals including honeybees, pigeons, salmon, and magnetoactic bacteria rely on iron, specifically magnetite (Fe_3O_4) for directional sense (Walker *et al.*, 1997).

Typical iron-bearing rocks include silicates (e.g., olivines) and sulfides (e.g., pyrite), in which iron is divalent ferrous iron. Iron is released into the environment by rock weathering. Iron oxides (e.g., ferrihydrite) are subsequently formed by oxidation and hydrolysis. Precipitation and dissolution of iron oxides depend heavily on pH, redox potential (Eh), temperature, and water activity of the environment. Under anaerobic conditions, iron oxides may be used by microorganisms as an electron acceptor and reduced (Lovley and Phillips, 1988). Through these processes and others, iron is ubiquitous in the environment.

Fe(III) is very insoluble in water, reaching concentrations of only about 10^{-12} M at pH 7.0, whereas Fe(II) is comparatively soluble, with concentrations on the order of 10^{-5} M in natural systems at pH 7.0 (Amonette, 2002). Thus, the oxidation state of iron significantly affects its mobility. Iron oxides form naturally in the environment and can

be very stable, in part due to the insolubility of ferric iron. Goethite (α-FeOOH) and hematite (α-Fe_2O_3) are the most stable iron oxides in most environments, but others exist in smaller quantities or in more extreme environments. Ferrihydrite, for example, is a precursor of goethite and hematite. It is widespread in nature, but not stable due to its high solubility and low crystallinity. Magnetite is a reduced iron oxide, containing both ferric and ferrous iron. As such, it is only common in reduced environments such as aquifers. Table 1 provides a list of iron oxides and their chemical formulas.

Magnetite

Magnetite is a mixed-valence iron oxide. One-third of the iron sites in magnetite are tetrahedrally coordinated with oxygen, while two-thirds are octahedrally coordinated, giving magnetite an inverse spinel structure. Tetrahedral sites are occupied by ferric iron, Fe(III), and octahedral sites can be occupied by both ferric and ferrous iron.

The ferrous to ferric iron ratio ($x = Fe^{2+}/Fe^{3+}$) of magnetite varies with the extent of oxidation of magnetite. Fully oxidized magnetite, which contains no ferrous iron ($x = 0$), is known as maghemite and has the chemical formula γ-Fe_2O_3. Stoichiometric magnetite ($x = 0.5$) contains equal amounts of ferrous and ferric iron in the octahedral sites and has the chemical formula Fe_3O_4.

Magnetite is ferromagnetic, which gives it many industrial applications including digital recording and drug delivery. Magnetite forms in nature through abiotic oxidation of ferrous minerals (Stratmann *et al.*, 1983) and biotic reduction of ferric oxides (Hansel *et al.*, 2005). It can also be formed through lithogenic processes.

Goethite

Goethite is a stable iron oxyhydroxide with the chemical formula α-FeOOH. Because of its stability, it is one of the more common iron oxides and provides a yellow-orange color to soils around the world. Goethite formation includes direct precipitation via nucleation/ crystal growth and transformation of ferrihydrite.

Interaction of Contaminants with Iron Oxides

Magnetite is well-documented as being a very strong adsorbent of arsenic (Dixit and Hering, 2003; Mayo *et al.*, 2007) as well as other contaminants. Magnetite has been found to reduce many environmental contaminants, including the nitrobenzene (Gorski and Scherer, 2009), carbon tetrachloride (Vikesland *et al.*, 2007; Danielson and Hayes, 2004), hexavalent uranium (Charlet *et al.*, 1998), and hexavalent chromium (Peterson *et al*., 1997). There is, however little data available on the reduction of arsenic by magnetite.

Goethite is also capable of adsorbing metals and contaminant anions (e.g., arsenic, chromium, lead, mercury, and selenium) in the environment (Waychunas *et al*., 2005).Goethite alone is not a viable reductant, but studies have shown that Fe(II)/goethite systems lead to fast reduction of environmental contaminants (Williams and Scherer, 2004).

Arsenic in the Environment

Arsenic is a naturally occurring metalloid and is widely distributed throughout the environment. It is present in biota, the atmosphere, oceans, lakes, groundwater,

sediments, and soils throughout the world. Four oxidation states are possible for arsenic: As(-III), As(0), As(III), and As(V). Elemental arsenic is rare in the environment. Arsine (AsH_3) is a flammable gas which has been detected emanating from anoxic environments (Cullen and Reimer, 1989). Crustal arsenic is most commonly found in sulfide minerals including arsenopyrite (FeAsS), orpiment (As_2S_3), and realgar (AsS). In aquatic systems, inorganic arsenite (AsO_3^{3-}) and arsenate (AsO_4^{3-}) are the most prevalent forms, although methylated arsenic species are generated by aquatic biota in trace concentrations (Oremland and Stolz, 2003).

Causes of Arsenic Mobilization

As discussed previously, arsenic is present in many minerals. In order to be available and reactive in aquatic environments and the atmosphere, arsenic must be mobilized. Arsenic mobilization has both natural and anthropogenic causes. Natural sources of arsenic mobilization include weathering of arsenic-bearing rocks, biological activity, and volcanic eruption. Anthropogenic sources include mining of metal ores (e.g., gold), combustion of fossil fuels, pesticide use, livestock feed additives, wood preservatives, and pigment production.

As seen in Figure 1, from Hindmarsh and McCurdy's 1986 review of arsenic toxicity, anthropogenic causes of arsenic mobilization outweigh natural causes. In most cases of groundwater contamination, however, a combination of natural and anthropogenic actions leads to arsenic release. This will be reviewed in more detail in the discussion of Bangladesh.

Arsenic Sorption

As(V) and As(III) exist as oxyanions in groundwater (i.e., AsO_4^{3-} and AsO_3^{3-}). As such, they adsorb readily to positively charged surfaces. Arsenic has been observed to sorb onto clays (Frost and Griffin, 1977; Goldberg and Glaubig, 1988). Sorption of arsenic onto iron oxides has been shown by several researchers (Fuller *et al.*, 1993;Waychunas *et al.*, 2005). Adsorption onto aluminum oxides, manganese oxides, and carbonate minerals has also been studied, though it occurs to a lesser extent (Sadiq, 1997; He and Hering, 2009).

Both arsenate and arsenite experience changing degrees of protonation with changing pH. Protonation of the species affects the charge, with fully-protonated species having zero charge and depronated species having negative charge. Figure 2, provided by Smedley and Kinniburgh (2002), depicts the speciation diagrams for both arsenite and arsenate. As seen in Figure 2, arsenite does not become negatively charged until pH ~9. Arsenate is negatively charged at much lower pH values (starting at pH ~3). The acid dissociation reactions of arsenate and arsenite are written along with corresponding pK_a values in Equations 1 – 5 (Goldberg and Johnston, 2001).

$$H_3AsO_4{}^0 \rightarrow H_2AsO_4{}^- + H^+ \qquad pK_{a,1} = 2.3 \qquad \text{Eq.1}$$

$$H_2AsO_4{}^- \rightarrow HAsO_4{}^{2-} + H^+ \qquad pK_{a,2} = 6.8 \qquad \text{Eq.2}$$

$$HAsO_4{}^{2-} \rightarrow AsO_4{}^{3-} + H^+ \qquad pK_{a,3} = 11.6 \qquad \text{Eq.3}$$

$$H_3AsO_3{}^0 \rightarrow H_2AsO_3{}^- + H^+ \qquad pK_{a,1} = 9.2 \qquad \text{Eq.4}$$

$$H_2AsO_3{}^- \rightarrow HAsO_3{}^{2-} + H^+ \qquad pK_{a,2} = 12.1 \qquad \text{Eq.5}$$

Arsenate and arsenite adsorption onto goethite and magnetite was studied by Dixit and Hering (2003). Their work showed that arsenate sorption decreases with increasing pH. Arsenite sorption trends are more complicated. As(III) desorption occurs at extreme pH values (both high and low) with an adsorption maximum occurring at approximately pH 9, which corresponds to its speciation diagram in Figure 2. Arsenate sorbs more strongly than arsenite, making arsenite the more mobile species.

Arsenic sorption increases with increases surface area of adsorbent. In natural systems, this can typically be interpreted to mean that arsenic sorption onto iron oxides on a mass of arsenic per mass of oxide basis can be ranked as follows: ferrihydrite>magnetite>goethite>hematite. Arsenic adsorption onto minerals can also be affected by other anions present in solution, such as phosphate (Gao and Mucci, 2001; Zhang and Selim, 2008).

Arsenic Redox Behavior

The reduction-oxidation (redox) chemistry of arsenic has been the subject of multiple studies. Arsenic redox behavior is of particular importance due to the increased toxicity and mobility of As(III) compared to As(V). Arsenate is the dominant form of arsenic in oxidized environments, whereas arsenite dominates in reduced systems as illustrated in Figure 3 (Smedley and Kinniburgh in 2002). Equations 6 – 12 show redox equations and potentials for relevant arsenic species.

$$H_3AsO_4{}^0 + 2H^+ + 2e^- \rightarrow H_3AsO_3{}^0 + H_2O \qquad E = +0.60\,V\ @\ pH = 0.0 \qquad \text{Eq. 6}$$

$$H_2AsO_4{}^- + 3H^+ + 2e^- \rightarrow H_3AsO_3{}^0 + H_2O \qquad E = +0.45\,V\ @\ pH = 2.3 \qquad \text{Eq. 7}$$

$$HAsO_4^{2-} + 4H^+ + 2e^- \rightarrow H_3AsO_3^0 + H_2O \qquad E = +0.08\,V\ @\ pH = 6.8 \qquad \text{Eq. 8}$$

$$HAsO_4^{2-} + 3H^+ + 2e^- \rightarrow H_2AsO_3^- + H_2O \qquad E = -0.22\,V\ @\ pH = 9.2 \qquad \text{Eq. 9}$$

$$AsO_4^{3-} + 4H^+ + 2e^- \rightarrow H_2AsO_3^- + H_2O \qquad E = -0.42\,V\ @\ pH = 11.6 \qquad \text{Eq. 10}$$

$$AsO_4^{3-} + 3H^+ + 2e^- \rightarrow HAsO_3^{2-} + H_2O \qquad E = -0.51\,V\ @\ pH = 12.7 \qquad \text{Eq. 11}$$

$$AsO_4^{3-} + 2H^+ + 2e^- \rightarrow AsO_3^{3-} + H_2O \qquad E = -0.60\,V\ @\ pH = 13.7 \qquad \text{Eq. 12}$$

Oxidation of As(III) by goethite has not been observed at neutral pH (Ona-Nguema *et al.*, 2005; Manning *et al.*, 2002; Amstaetter *et al.*, 2010). Neither has oxidation of As(III) by lepidocrocite (Ona-Nguema *et al.*, 2005; Manning *et al.*, 2002). However, oxidation of As(III) by oxygen was found to occur at Fe(II)-activated ferrihydrite and magnetite surfaces (Ona-Nguema *et al.*, 2010). Anoxic oxidation of As(III) by Fe(II)-activated goethite has also been observed (Amstaetter *et al.*, 2010).

Ramos *et al*. (2009) found that zero valent iron nanoparticles (nZVI) promote simultaneous As(III) oxidation to As(V) and As(III) reduction to As(0) due to the reducing potential of the ZVI and the oxidizing potential of the thin iron oxide layer that spontaneously forms around ZVI particles. As(III) oxidation by H_2O_2 has not been observed in the absence of ferric iron, but is a strong oxidant in the presence of ferric iron (Voegelin and Hug, 2003). Other metal oxides are also capable of oxidizing As(III). Both biogenic and synthetic manganese oxides have been shown to oxidize As(III) (Tani *et al.*, 2003).

Oremland and Stolz (2003) discussed two types of As(III) oxidizing prokaryotes: heterotrophic arsenite oxidizers (HAOs) and chemolithoautotrophic arsenite oxidizers

(CAOs). HAOs have been suggested to oxidize arsenite as a detoxification measure, whereas CAOs couple As(III) oxidation to oxygen reduction, promoting cell growth.

As(V) reduction by iron oxides has yet to be documented. Abiotic reduction of arsenate has been shown to occur in the presence of humic acid (Palmer and von Wandruszka, 2010), fulvic acid (Tongesayi and Amart, 2007), and sulfide (Rochette *et al.*, 2000).As(V) reduction to As(III) and As(0) by nZVI was observed by Ramos *et al.* (2009).

Biotic reduction of arsenate by anaerobic respiration of dissimilatory arsenic-reducing bacteria isolated in the laboratory has been observed (Yamamura *et al.*, 2003). Oremland and Stolz (2003) list 16 known DARBs, though no obligate DARBs have been found.

Health Effects of Arsenic

As(III) is more toxic than As(V) due to the difference in their metabolic pathways. As(III) quenches the tricarboxylic acid (TCA) cycle by binding to thiols in pyruvate dehydrogenase. Arsenite binding to sulfhydryl groups also impairs the function of many proteins (National Research Council, 1999). As(V) competes with phosphate, inhibiting the production of adenosine triphosphate (ATP) which transports energy within cells (Oremland and Stolz, 2003). These pathways are associated with noncancerous effects of arsenic exposure.

Arsenic is a known carcinogen recognized by the Environmental Protection Agency (EPA). Due to widespread arsenic contamination, epidemiological studies in many countries including Taiwan and Chile show that chronic ingestion of high

concentrations of As(III) and/or As(V) causes bladder, lung, and skin cancer (National Research Council, 1999). Noncancerous effects of prolonged arsenic exposure include skin lesions and peripheral vascular disease.

The half-life of arsenic in the body is approximately four days. The main loss pathway for arsenic in the body is excretion through urine (IARC, 2004). Humans and other animals are known to methylate inorganic arsenic, causing it to be less toxic and more readily excreted.

Guidelines and Regulation of Arsenic

The World Health Organization (WHO) develops Guidelines for Drinking Water Quality (GDWQ) in order to protect public health from drinking water contaminants. The 1993 edition of WHO GDWQ established the arsenic drinking water guideline of 10 µg/L (10 ppb). This guideline is significantly lower than the 50 µg/L provided in 1984 due to the high lifetime skin cancer risk observed in Taiwan.

The United States Environmental Protection Agency (EPA) set the maximum contaminant level (MCL) for arsenic at 10 µg/L in January 2001. Before 2001, the MCL was 50 µg/L. Currently, the arsenic limit in Bangladesh is set to 50 µg/L (UNICEF, 2008).

An Epidemic: Arsenic Contamination in Bangladesh

Before 1970, Bangladesh's main source of drinking water was from rivers, lakes, and ponds. These waters were (and remain) contaminated with agricultural, industrial,

domestic, and municipal wastes. Drinking and waste water treatment remains largely nonexistent in Bangladesh due to limited monetary resources as well as regular droughts.

In the 1970's, tube well installation began in the hopes that the country could tap into their groundwater resources and circumvent the health issues involved with drinking surface water. Currently, an estimated 95% of the Bangladeshi population drinks from well water sources. Due to a coupling of natural and anthropogenic causes, however, arsenic levels in the aquifers of Bangladesh reach concentrations as high as 2.5 mg/L (Nordstrom, 2002) and commonly exceed 50 µg/L, the Bangladesh limit for arsenic (Chakraborti *et al.*, 2002). An estimated 70 million people are currently drinking contaminated well water. This contamination problem has led to arsenicosis in millions of Bangladeshis, and the issue has yet to be resolved. Figure 4 is taken from Chakraborti's 2002 study of arsenic contamination in Bangladesh. The figure shows the large extent of the arsenic problem. Table 2 displays arsenic concentration distributions in tube wells of Bangladesh and West Bengal, India (Rahman *et al.*, 2001).

Two major theories for the cause of arsenic contamination have been established. The source of arsenic is the same for both theories, as arsenic is naturally present in the sediment of aquifers in Bangladesh. Arsenic can be in sulfide minerals, such as arsenopyrite, or adsorbed/coprecipitated with Fe oxides and clays. The cause of mobilization is thought to be one of the following:

(1) Surface waters are contaminated with organic carbon originated from agricultural and municipal wastes. High groundwater withdrawal rates due to drought and irrigation causes surface waters to recharge the groundwater. In the aquifer, the organic carbon either reduces and dissolves iron on its own or is used as an electron

donor by dissimilatory iron reducing bacteria (DIRB) which use iron as an electron acceptor, leading to reduction and dissolution of iron minerals. As iron dissolves into solution, any arsenic adsorbed onto or coprecipitated with the mineral is released into the groundwater (Nickson *et al.*, 2000).

(2) Groundwater levels drop due to drought and irrigation. This leads to aeration of the previously anoxic groundwater. Thus, arsenopyrite becomes oxidized and dissolves, releasing arsenic to the groundwater (Mandal *et al.*, 1998).

Arsenic Contamination in the United States

Cases of arsenic contamination have been documented in the United States since the late 1970's. Many of these contaminations are due to acid mining of gold, lead, zinc, and other metals. Mining-induced elevated groundwater arsenic concentrations have been observed in Alaska (Wilson and Hawkins, 1978), Idaho (Mok and Wai, 1990), California (Webster *et al.*, 1994), Nevada (Grimes *et al.*, 1995), Montana (Welch *et al.*, 2000), and South Dakota (Ficklin and Callender, 1989).

Natural dissolution and desorption as well as geothermal waters can also lead to arsenic concentrations exceeding the EPA standard. States in which natural processes have resulted in elevated arsenic concentrations include Maine, Michigan, Minnesota, Oklahoma, and Wisconsin (Smedley and Kinniburgh, 2002). Figure 5 highlights regions in the US that have arsenic concentrations exceeding 50 µg/L (Welch *et al.*, 2000).

Arsenic Contamination in Iowa

The University of Iowa Center for Health Effects of Environmental Contamination (CHEEC) performed a statewide analysis of rural well water (SWR2) in 2009 as a follow-up to a previous study. In the study, 473 private rural wells were sampled and tested for arsenic. Of these wells, 48% tested above the maximum detection limit (MDL) of 1 µg/L and 8% exceeded the EPA MCL of 10 µg/L (CHEEC, 2009). An arsenic speciation study was also performed using an HPLC-ICP-MS. It was found that up to 75% of the total arsenic concentration in water samples was in the form of inorganic As(III).Figure 6shows the location and concentration range of the 226 wells that contained detectable levels of arsenic.

Table 3 breaks arsenic detections in Iowa into sampling regions. Arsenic concentrations are highest in north-central rural wells. In 2005, Erickson and Barnes attributed the elevated arsenic concentrations of the Midwest to the late Wisconsinan glacial drift, which encompassed north-central Iowa but no other region in the state (Figure 7).

Treatment Methods for Arsenic-Contaminated Water

Several treatment methods for arsenic-contaminated drinking water have been investigated, with an increased interest in development occurring recently due to the arsenic epidemic in Bangladesh. The main mechanism of removal used is precipitation/coprecipitation. Other treatment methods include membrane filtration, adsorption, ion exchange, and permeable reactive barriers (PRBs).

Mohan and Pittman, Jr. (2007) compiled a review of several papers using different adsorbents to remove arsenic from solution. According to their review several iron-containing media have been tested including goethite, ferrihydrite, hematite, iron oxide granular activated carbon (GAC), and iron oxide coated sand. Recently, magnetite has been tested for its feasibility as an adsorbent (Mayo *et al.*, 2007).

Goals and Hypotheses of Present Study

The initial goals of this work were to implement a method for determining arsenic concentration and oxidation state using the inductively-coupled plasma mass spectrometer (ICP-MS) and cartridges containing an As(V)-selective anionic exchange resin. The subsequent goals of the study were to validate the counterintuitive results of Amstaetter *et al.* (2010)and to evaluate whether magnetite is capable of reducing As(V). The findings of the 2010 study by Amstaetter *et al.* showed oxidation of arsenite to arsenate in the presence of Fe(II)-activated goethite despite thermodynamic predictions that As(V) would be reduced to As(III).

1. Implement arsenic analytical method with ICP-MS.
2. Implement method to distinguish between As(III) and As(V).
3. Confirm As(III) oxidation by Fe(II)-activated goethite observed by Amstaetter *et al.* (2010)
4. Evaluate potential for arsenate reduction by magnetite.

Table 1. Names and Formulas of Common Iron Oxides

Mineral	**Formula**
Ferrihydrite	$Fe_5HO_8 \cdot 4H_2O$
Goethite	α-FeOOH
Hematite	α-Fe_2O_3
Lepidocrocite	γ-FeOOH
Maghemite	γ-Fe_2O_3
Magnetite	Fe_3O_4

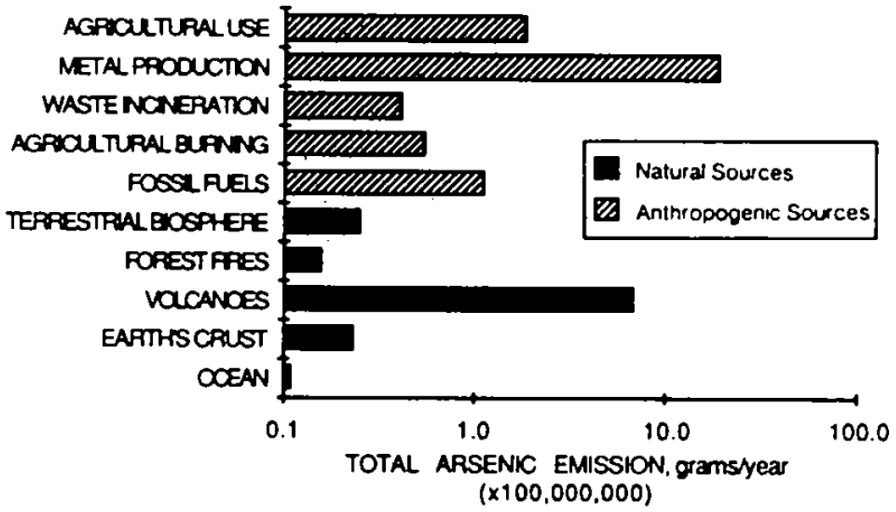

Figure 1. Global Arsenic Emissions

(Hindmarsh and McCurdy, 1986)

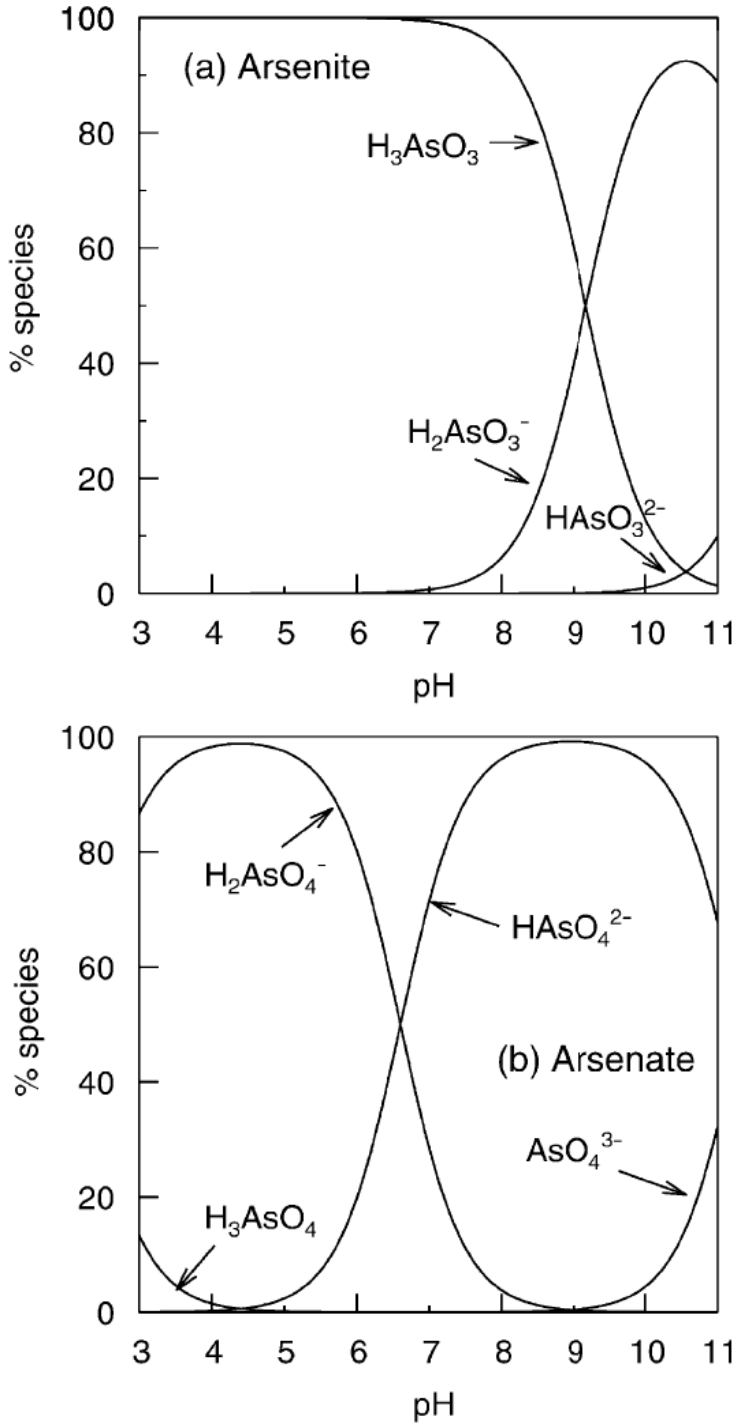

Figure 2. Speciation Diagram for Arsenite and Arsenate

(Smedley and Kinniburgh, 2002)

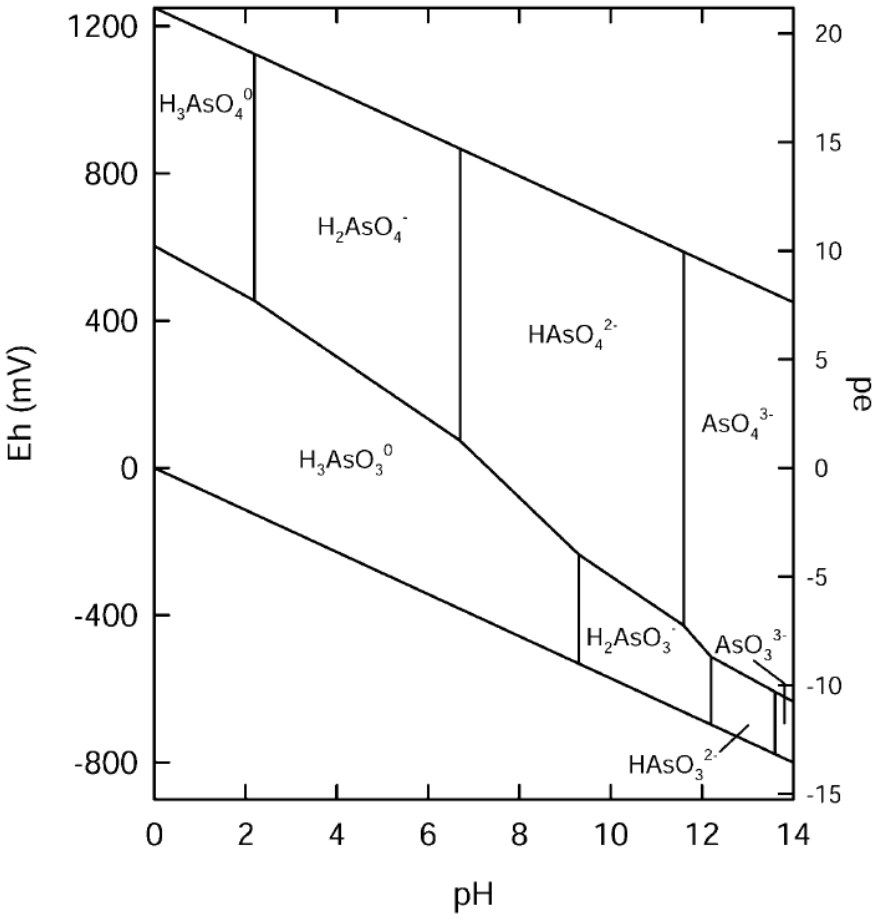

Figure 3. Eh-pH Diagram for Arsenic

(Smedley and Kinniburgh, 2002)

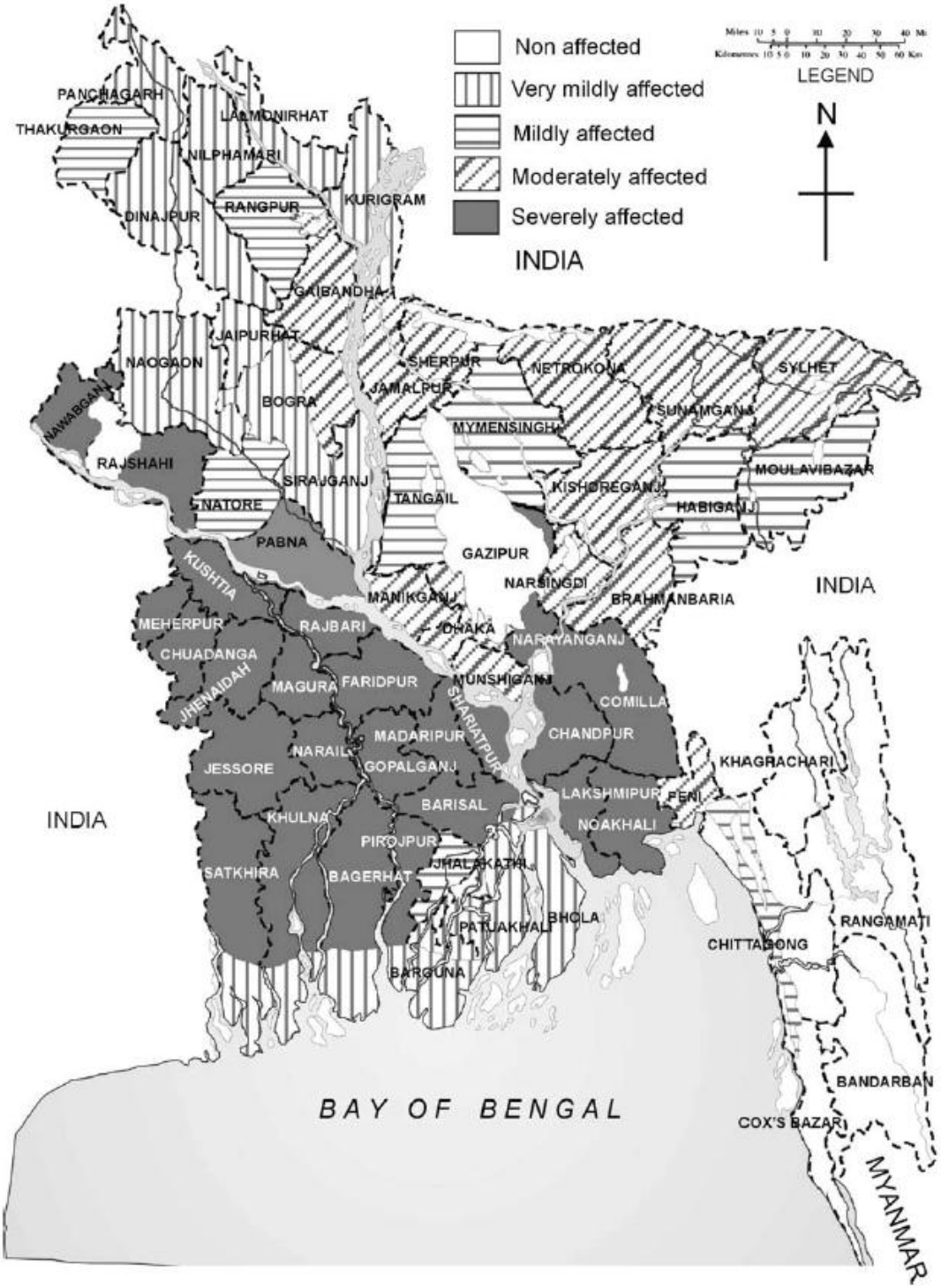

Figure 4. Degree of Arsenic Contamination in Bangladesh

(Chakraborti *et al.*, 2002)

Table 2. Arsenic Distribution in Tube Wells of Bangladesh and West Bengal, India

Country	Total Water Samples Analyzed	Distribution of Total Samples by Arsenic Concentration (µg/L)							
		<10	10–50	51–99	100–299	300–499	500–699	700–1000	>1000
Bangladesh	34,000	14,991 (44.1%)	6429 (18.9%)	2949 (8.7%)	5812 (17.1%)	2174 (6.4%)	894 (2.6%)	479 (1.4%)	272 (0.8%)
West Bengal, India	101,934	49,310 (48.4%)	27,309 (26.8%)	10,005 (9.8%)	11,782 (11.6%)	2354 (2.3%)	724 (0.7%)	334 (0.3%)	116 (0.1%)

Source: Rahman *et al.* (2001). Chronic Arsenic Toxicity in Bangladesh and West Bengal, India – A Review and Commentary. *Journal of Toxicology-Clinical Toxicology*, 683-700.

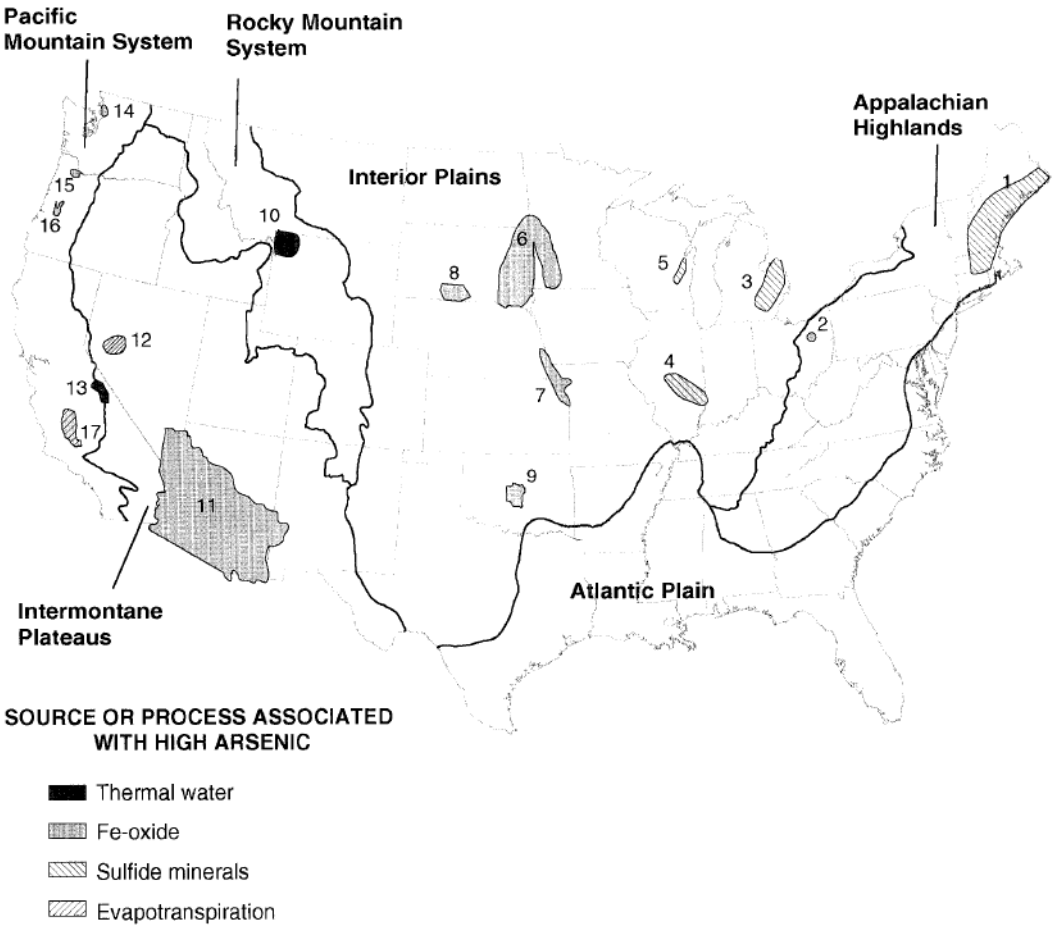

Figure 5. Regions in the US with As Concentration > 50 µg/L

(Welch *et al*., 2000)

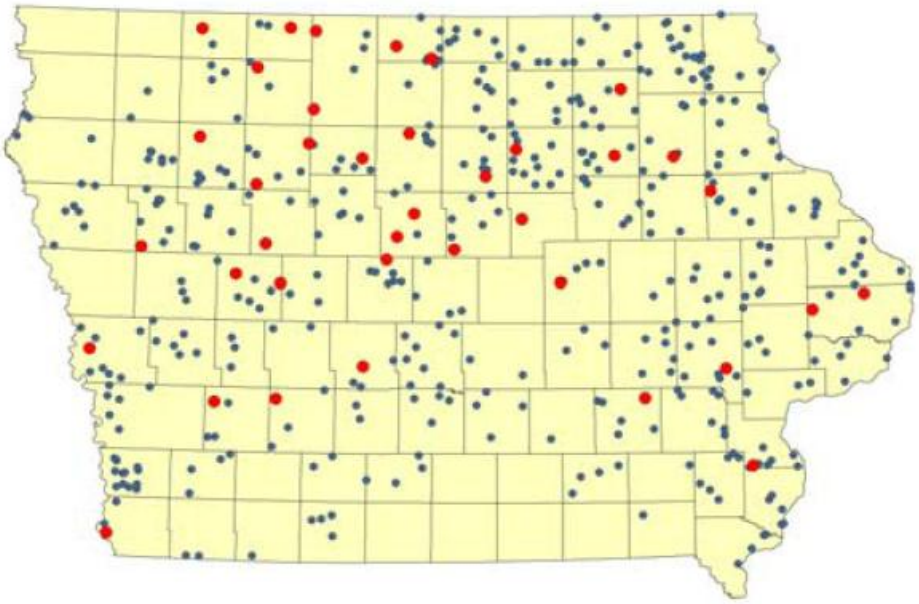

Figure 6. SWRL2 Arsenic Detection Levels

Red/large dots ≥10 µg/L; blue/small dots 1-9 µg/L. (CHEEC, 2009)

Table 3. SWRL2 Arsenic Concentration by Sampling Region

Sampling Region	Arsenic Concentration (mg/L) <0.001	0.001 - <0.01	≥ 0.01	Total
East-central	89	56	9	154
North-central	39	43	19	101
Northeast	58	20	3	81
Northwest	13	17	1	31
South-central	23	16	1	40
Southwest	25	35	6	66
Total	247	187	39	473

Source: CHEEC. (2009). *Iowa Statewide Rural Well Water Survey Phase 2 (SWRL 2) Results and Analysis*. Iowa City, IA: The University of Iowa.

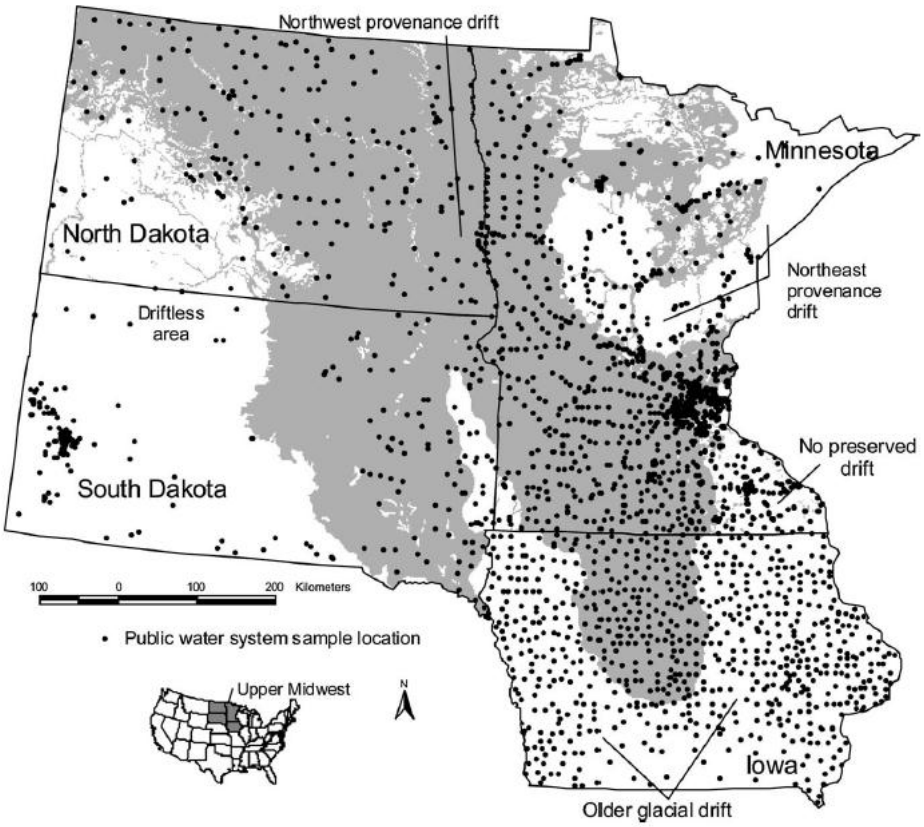

Figure 7. Northwest Provenance Drift

(Erickson and Barnes, 2005)

CHAPTER II ARSENIC ANALYSIS

Introduction

There has been a shift in arsenic analysis methods with the advent of more sensitive methods such as the inductively coupled plasma mass spectrometer (ICP-MS). Gaseous hydride atomic absorption (GHAA) spectroscopy and inductively coupled plasma optical emission spectrometry (ICP-OES) are both capable of determining arsenic concentration. However, the EPA no longer approves of the ICP-OES for the determination of arsenic concentration in water samples, due to its low resolution compared to that of the ICP-MS. The ICP-OES has a method detection limit (MDL) of 8 µg/L for aqueous arsenic, whereas the ICP-MS has an MDL six times lower, at 1.4 µg/L. GHAA has the lowest MDL at 0.5 µg/L (EPA, 1999).

ICP-MS Background

Inductively coupled plasma mass spectrometry (ICP-MS) is a high resolution technique that can analyze both simple and complex matrices for trace elements. The ICP-MS works by first introducing the sample into an argon (Ar) stream. The sample is nebulized by Ar gas then ionized by Ar plasma. The ions then travel through an interface that takes them from the atmospheric pressure and elevated temperature (~6000 K) of the plasma torch to the room temperature and high vacuum (10^{-4} – 10^{-3} torr) of the mass spectrometer. The plasma then passes through two nickel cones with millimeter-sized orifices, during which most of the argon atoms are removed by a vacuum pump. Next, the ions are focused into the mass spectrometer with a lens and separated by their mass to

charge ratio (m/z) with a quadrupole. The user first selects the atom and isotope to be studied and quadrupole enables only ions with the mass to charge ratio characteristic of the isotope of interest to reach the detector. The detector uses an electron multiplier to obtain a count per second value for the selected isotope (Shilling and Kingsley, 2001).

The mass to charge ratio is a reasonably good indicator of the atom being studied, but interferences by other compounds may overestimate the concentration of the element of interest. Also, it is critical that the user have a good idea of the concentration of the analyte in a sample before running it on the ICP-MS. Because the instrument is meant to measure very low concentrations, it can easily be overwhelmed by part per million (ppm) quantities. In this case, there is prolonged retention of the ions in the instrument and cross contamination of samples may occur. High concentrations are also harmful to the detector. If a sample is known to have a high concentration of analyte and dilution is not desired, it is sometimes possible to choose a less abundant isotope of the analyte for analysis, which will reduce the number of ions of the given mass to charge ratio reaching the detector.

Arsenic only has one stable isotope, ^{75}As, so this isotope was chosen to be analyzed by the ICP-MS. Interferences with ^{75}As on the ICP-MS include $^{1}H^{+74}Ge$ and $^{35}Cl^{+40}Ar$. Germanium did not occur in high concentrations in the samples analyzed, so interference caused by its coupling with hydrogen was not an issue in sample analysis. However, special care was taken not to introduce high concentrations of chloride into the samples analyzed by the ICP-MS. Because hydrochloric acid (HCl) is often used in the reductive dissolution of iron oxides, alternative methods had to be considered to preserve the quality of the data. Arsenic concentrations analyzed by the ICP-MS were typically in

the range of 0 – 100 µg/L. Maintaining low concentrations of arsenic in the samples prolongs the life of the detector while simultaneously producing a minimal amount of arsenic waste.

Materials

Stock Solutions

Arsenate stock solutions used in the experiments was made from sodium arsenate (Na_2HAsO_4) and deionized (DI) water. Arsenate solutions were found to remain relatively stable, with no detectable reduction to As(III) over the course of several months. Arsenite stock solutions were made from sodium arsenite ($NaAsO_2$) and DI water. Oxidation of As(III) to As(V) in arsenite stock solutions of 1 g/L was seen in a matter of weeks, requiring the preparation of new stock solutions for each set of experiments.

As(V)-selective Cartridges

As discussed previously, the oxidation state of many contaminants, including arsenic, affects the element's mobility and toxicity. As(III) is much more mobile and toxic than As(V), so studying arsenic redox reactions with iron oxides is crucial in determining arsenic's fate in the environment.

To determine the arsenic oxidation state of samples, cartridges produced by MetalSoft Center, NJ, USA were used. These cartridges employ an anionic exchange resin that selectively adsorbs arsenate while letting arsenite pass through the cartridge. Thus, arsenite concentration in a sample could be deduced by passing the solution

through a cartridge and measuring the arsenic concentration using the inductively coupled plasma mass spectrometer. Total arsenic concentration was measured on the ICP-MS with samples that were not passed through the cartridge. Arsenate concentration was calculated as the difference between total arsenic and arsenite concentrations (Equation 13). Shown in Figure 8 is a schematic of the sampling procedure used to identify As(III) and As(V) concentrations in a sample.

$$[As(V)]_{aq} = Tot_{As,aq} - [As(III)]_{aq} \quad \text{Eq. 13}$$

Arsenic Method Development

Arsenic concentrations were determined using a Thermo Scientific XSERIES ICP-MS. Isotopes of interest are read by the ICP-MS detector in counts per second (cps). In order to convert this to units of concentration, a standard curve was developed by analyzing arsenic samples of known concentrations. This was done for both arsenite and arsenate. Standards were run through the As(V)-selective cartridges to check for oxidation or reduction of the stock solutions. Figures 9 and 10 show standard curves for As(III) and As(V), respectively.

An internal standard of 10 µg/L rhodium was used to correct for drift in the instruments readings. Rh concentration was assumed to be equal in all solutions and arsenic cps was adjusted using the ratio of the Rh concentration of that sample to the Rh concentration of the initial sample. Equation 14 shows how the internal standard was used to standardize measured As concentrations.

$$[As]_{calculated} = [As]_{measured} \cdot \frac{[Rh]_{measured}}{[Rh]_{initial\ sample}} \quad \text{Eq. 14}$$

Combining the As(V)-selective cartridges with the ICP-MS, speciation and concentration of arsenic in experimental samples were determined. Validation of the effectiveness of the cartridges can be seen in Table 4.

Total As added to the samples was 50 µg/L. The mean and standard deviation of the total arsenic concentrations in Table 4 are 48±2.9 µg/L, which provides evidence for good mass balance on As recovery. Figure 11 plots measured As(III) concentration vs. nominal As(III) concentration. Figure 12 plots measured As(V) concentration vs. nominal As(V) concentration. There is a high correlation between measured and nominal As(III) and As(V) concentrations, indicating that the cartridges are effective at removing As(V) without removing As(III) from solution.

As shown in Figure 11, measured concentrations for As(III) ranged from 3 – 29% lower than expected As(III) concentrations. This is most likely due to a small fraction of As(III) being removed by the cartridges. The cartridges have been reported to provide 98% removal of As(V) and 95% recovery of As(III) (Meng *et al.*, 2001).

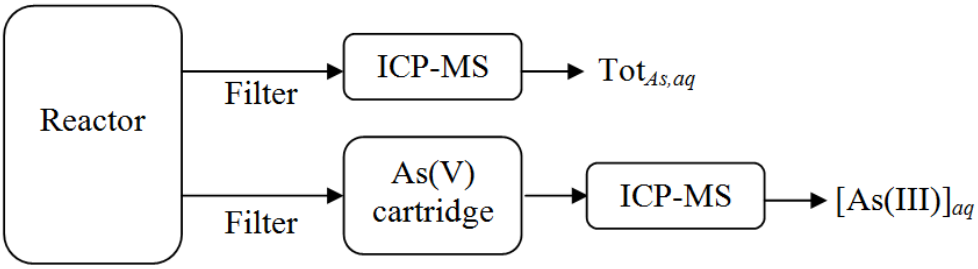

Figure 8. Sampling Procedure Schematic

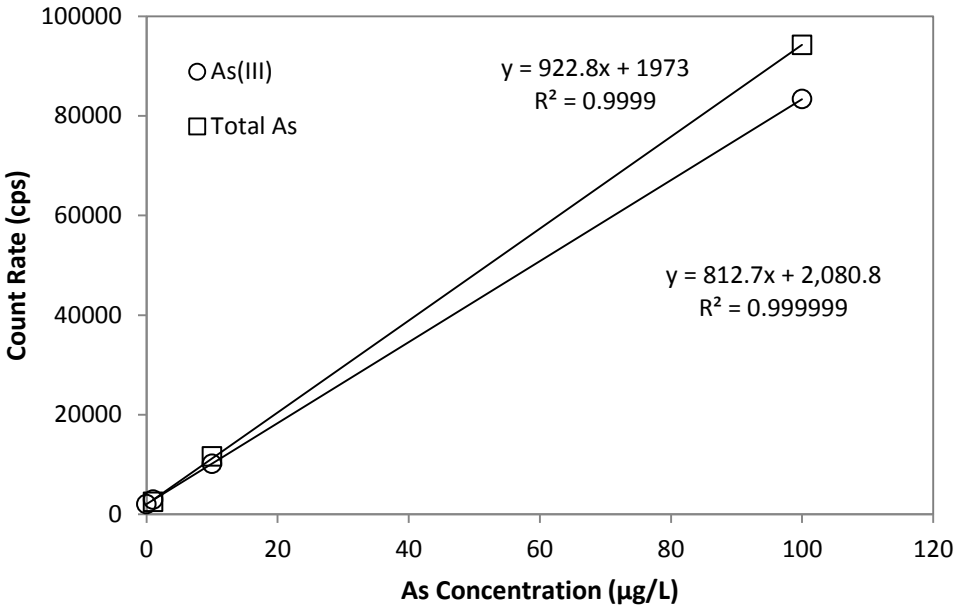

Figure 9.As(III) Standard Curve

Sodium arsenite ($NaAsO_2$) was used to make the standards. Total As was determined from a filtered sample with drift correction based on the Rh internal standard. As(III) was determined from a filtered sample run through an As(V)-selective cartridge with drift correction based on the Rh internal standard.

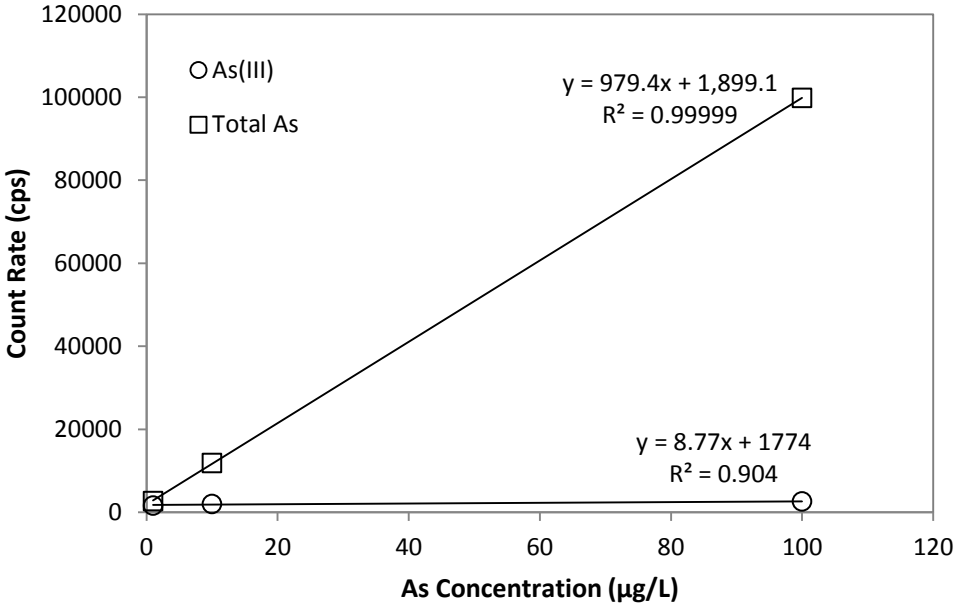

Figure 10.As(V) Standard Curve

Arsenate salt (Na_2HAsO_4) was used to make the standards. Total As was determined from a filtered sample with drift correction based on the Rh internal standard. As(III) was determined from a filtered sample run through an As(V)-selective cartridge with drift correction based on the Rh internal standard.

Table 4. Cartridge Efficiency as Measured by the ICP-MS

Concentration Added		Concentration Measured		Calculated
As(III) (µg/L)	As(V) (µg/L)	As(III) (µg/L)	Tot As (µg/L)	As(V) (µg/L)
0	50	0.02	50.8	50.8
10	40	7.13	52.2	45.1
20	30	15.7	47.9	32.2
30	20	23.4	47.8	24.5
40	10	32.8	45.2	12.4
50	0	48.3	45.1	-3.2

Note: [As(V)] = Tot As – [As(III)]
Tot As = 48±2.9 µg/L

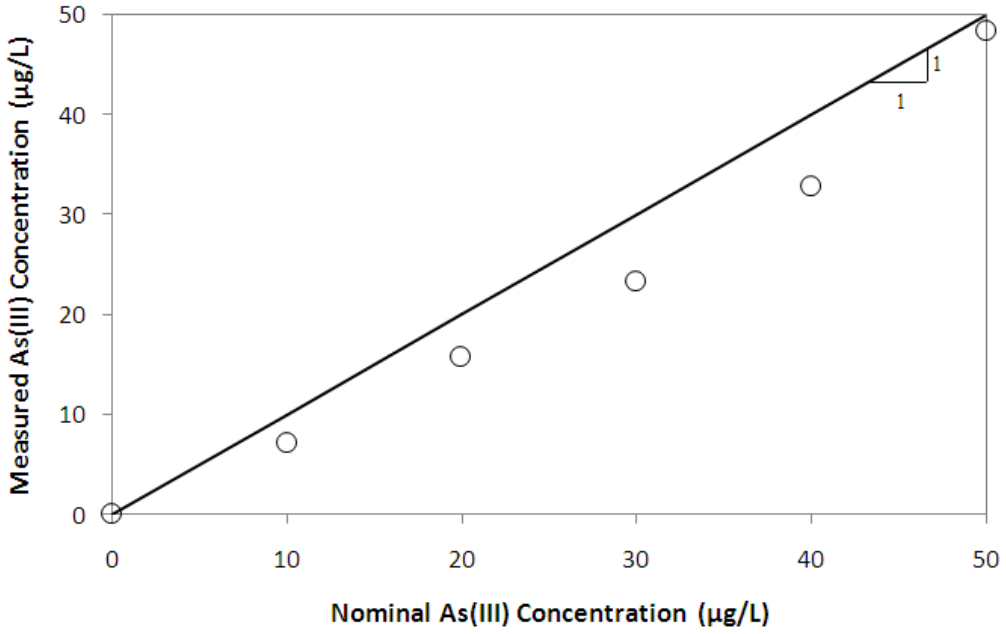

Figure 11. Measured vs. Nominal As(III) Concentration after Filtration through Cartridge

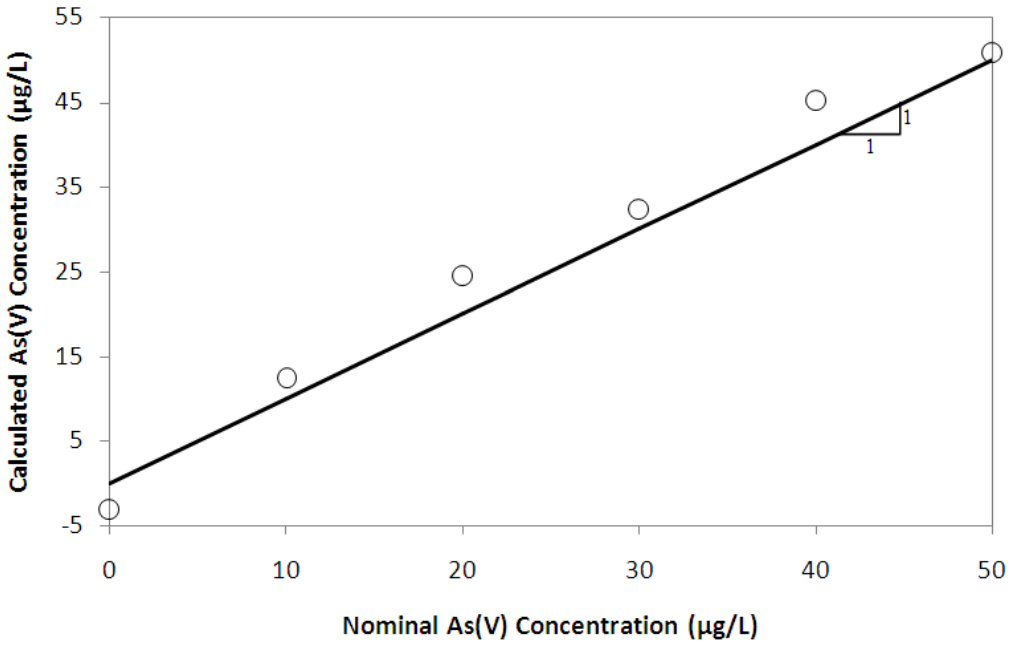

Figure 12. Calculated vs. Nominal As(V) Concentration after Filtration through Cartridge

CHAPTER III OXIDATION OF AS(III) BY FE(II)/GOETHITE

Introduction

The experiments discussed in this chapter were meant to mimic those of Amstaetter *et al.* (2010). Goethite with or without aqueous Fe(II) was reacted with As(V) and As(III) in order to observe adsorption and redox reactions. The goal of the experiments was to confirm the oxidation of As(III) by goethite + Fe(II) observed by Amstaetter *et al.* (2010) because this result is highly non-intuitive.

The goethite suspension preparation and reactor set-up described in the Methods section of this chapter were based off of the methods used by Amstaetter *et al.* (2010). The main difference between the conditions of their experiments and of ours was the specific surface area of the goethite used. They used a manufactured Bayferrox goethite with a specific surface area of only 9.2 m^2/g, while the goethite used in our experiment had a much higher surface area of 33 m^2/g.

Amstaetter *et al.* (2010) used ICP-MS, As(V)-selective cartridges, and XAS to determine aqueous arsenic concentration, aqueous arsenic oxidation state, and adsorbed arsenic oxidation state, respectively. They did not show mass balance of arsenic in the system, but rather took the adsorbed concentration to be the difference between the initial and final aqueous arsenic concentration.

Results provided by Amstaetter *et al.* (2010) showed no redox transformation in the goethite + As(III)/As(V) samples. Previous research has shown that goethite alone is relatively inactive in redox processes (Klausen *et al.*, 1995; Fredrickson *et al.*, 2000), so these results were expected. However, the group also showed that As(V) was not

reduced by goethite + Fe(II) systems while As(III) was oxidized by the system. This result is highly non-intuitive, as thermodynamic predictions and previous research suggests that Fe(II)/goethite systems are reductive rather than oxidative (Klausen *et al.*, 1995; Amonette *et al.*, 2000). Because most of the arsenic in their experiments was adsorbed to goethite, XAS data can be used to determine extent of redox reactions taking place in the samples. Figure 13 shows the Amstaetter *et al.* (2010) As-XANES data for all of the experimental conditions tested.

Amstaetter *et al.* (2010) posed that a reactive Fe(III) intermediate was formed after Fe(II) sorption onto goethite and was responsible for the subsequent As(III) oxidation. A schematic of the formation of the reactive Fe(III) intermediate and the pathway for As(III) oxidation are shown in Figure 14. Our intent was to confirm arsenite oxidation by Fe(II)/goethite

Methods

Goethite Synthesis

Goethite synthesis followed procedures outlined by Schwertmann and Cornell in Iron Oxides in the Laboratory (2000). First, 100 mL of a 1 M $Fe(NO_3)_3$ solution was prepared by dissolving $Fe(NO_3)_3 \cdot 9H_2O$ in DI water. A 180 mL solution of 5 M KOH was added rapidly to the $Fe(NO_3)_3$ solution while stirring. Mixing of these two solutions formed a reddish brown precipitate, ferrihydrite. This was diluted to a final volume of 2 L with DI water. The suspension was then heated at 70^{o}C for roughly 60 hours. After heating, the solution was yellow, signifying that goethite had formed. The precipitate

was then centrifuged and washed with DI several times. The clean goethite was freeze dried and sieved through a 100 mesh sieve.

Goethite Characterization

The BET, named after its developers: Brunauer, Emmett, and Teller, was used to determine the specific surface area of the synthesized iron oxides. The BET measures N_2 gas adsorption onto the dehydrated solid surface at liquid nitrogen temperature. Mass of N_2 gas adsorbed can then be measured, and volume of pore space (assumed to be equal to gas volume) can be calculated. Goethite used in the following experiments was found to have a specific surface area of 33 m^2/g.

Powder x-ray diffraction (pXRD) with a cobalt source was used to verify the crystal structures of the prepared goethite. Each iron oxide has a characteristic diffraction pattern which can be compared to the diffraction pattern produced by the synthesized iron oxide. No impurities were found in the synthesized goethite using this method. X-ray diffractograms can be used to estimate particle size with the Scherrer equation. Figure 15 shows the diffractogram produced by the goethite sample along with goethite's characteristic diffraction pattern.

Transmission electron microscopy (TEM) was used to image the goethite particles. The synthesized goethite was found to be acicular, which further confirms that goethite was formed in the synthesis process. Micrographs can also be used for particle sizing. Particle length and width can be used to estimate specific surface area with a few assumptions regarding the three dimensional shape of the particle. A micrograph taken of the prepared goethite is shown in Figure 16.

Mössbauer spectroscopy can be used to determine the oxidation state and structure of iron oxides in solid samples. Mössbauer spectroscopy uses recoilless gamma ray absorption to measure changes in the energy levels of atomic nuclei. Of the iron isotopes, Mössbauer spectroscopy can only read ^{57}Fe due to the presence of a nuclear spin in this and no other iron isotope.

Goethite Suspension Preparation

As described by Amstaetter *et al.*, a suspension of 50 m^2/L goethite was prepared in deoxygenated deionized water in a glovebox containing 93% nitrogen and 7% hydrogen gas. Based on the BET results discussed previously, the surface area concentration was converted to a goethite loading of 1.5 g/L. The suspension was allowed to mix for at least 24 hours before adjusting the pH to a value of 7.0 using 0.2 M NaOH. After the pH stabilized, which took approximately two days, aliquots were taken and arsenic spikes were added.

For the Fe(II)-activated goethite samples, an aqueous Fe(II) concentration of 1 mM was attained by adding roughly 1.18 mM Fe(II) to the goethite suspension. Excess Fe(II) was required in the system due to Fe(II) sorption onto goethite particles. Fe(II) addition required additional NaOH to maintain a pH of 7.

Reactor Set-up

All experiments were performed at room temperature in a glovebox. 60 mL reactor vials were wrapped in aluminum foil to prevent photochemical reactions and filled with 50 mL of goethite suspension. An arsenic concentration of 2 mg/L was added to each

reactor vial. All sample conditions were prepared in triplicates. Conditions tested included:

1. Goethite + As(III)
2. Goethite + As(V)
3. Goethite + Fe(II) + As(III)

Sampling Method

Goethite interactions with arsenite and arsenate were allowed to proceed for seven days before sampling. The Fe(II)/goethite + As(III) samples were sampled after zero hours, six hours, and seven days of mixing. Samples were first run through a 0.45 μm nitrocellulose filter to remove solids. Half of the filtered solution was passed through an As(V)-selective cartridge to remove As(V) as discussed previously. 4.5 mL of the cartridge and non-cartridge samples was placed into a plastic ICP-MS sample tube along with 0.5 mL 1 N HNO_3 (added for sample stability) and 1 mL 50 μg/L rhodium (added as an internal standard). All samples were stored at 4^oC in a refrigerator until analysis on the ICP-MS.

Aqueous iron concentration and composition was determined using the 1,10-phenanthroline method (Schilt, 1969). Sample absorbance was read on a UV-vis spectrophotometer at a wavelength of 510 nm.

Analysis Method

As discussed previously, the ICP-MS was used to determine aqueous arsenic concentration in all samples. The spectrophotometer was used to determine aqueous iron

concentration using the 1,10-phenanthroline method. The X-ray absorption spectrometer (XAS) was used to analyze adsorbed arsenic oxidation state. The following is a brief description of XAS:

X-ray absorption spectroscopy (XAS) is a useful tool for studying the local structure around elements within a material. XAS can be performed on crystals, amorphous solids, liquids, and molecular gases. Solid-state XAS was used in these experiments due to the difficulties associated with maintaining arsenic oxidation state during extraction of arsenic from the solid phase. X-ray absorption near edge spectroscopy (XANES) was used to determine the speciation of arsenic adsorbed to the iron oxide surface. This information was particularly useful due to the large extent of adsorption witnessed in the experiments.

XAS measures the X-ray absorption coefficient, u, which describes the extent of X-ray absorption and is measured in terms of energy. The absorption coefficient decreases with increasing X-ray energy, except at specific energies where a sudden increase in absorption occurs. These spikes in absorption are termed X-ray absorption edges and the energies at which they occur are characteristic to the atoms in the sample. These energies correspond to the binding energies of electrons, or the energy required to excite an electron from a low-energy state to a higher-energy state in an atom. Using preexisting knowledge on binding energies of the atoms, XAS data can be interpreted to provide information on the composition of the sample (Bunker, G., 2010).

Results

Based on the data collected by Amstaetter *et al.* (2010), As(III) oxidation by the Fe(II)/goethite system was expected. No oxidation of arsenite or reduction of arsenate was expected to occur in the goethite systems without Fe(II) addition.

At least 80% of the arsenic sorbed onto goethite particles in all of the experiments. Some oxidation of As(III) was observed in the goethite + As(III) samples, however[As(V)] was 1.3 µg/L, whereas the method detection limit (MDL) was 1.55µg/L, assuming a 90% confidence interval (CI). Results for the goethite + As(III) and goethite + As(V) experiments are shown in Table 5. Amstaetter *et al*. data is provided within the table for ease of comparison.

There was some evidence for As(III) oxidation in the Fe(II)/goethite system, as seen in Figure 17. A majority of the arsenic did sorb however, making it difficult to draw conclusions from the aqueous phase composition.

Data provided in Figure 17 is displayed in terms of percent of total aqueous arsenic in Figure 18. There was a high degree of similarity between the data collected for this study and the data presented by Amstaetter *et al*. (2010) especially in terms of percent of total concentration.

XAS data was provided for the solid samples by the Argonne National Laboratory. The results can be seen in Figure 19. No reduction of arsenate by goethite was seen, as demonstrated by the fact that the peak of the goethite + As(V) sample does not shift from the electron binding energy of the As(V) standard solution to the energy of the As(III) standard solution. There is some evidence for arsenite oxidation by both the goethite and Fe(II)/goethite systems. This is seen in the reduced As(III) peaks for these

samples compared to the As(III) solution standard. However, a corresponding increase in As(V) peak was not observed for these samples, so arsenite oxidation cannot be verified. These results differ from those of Amstaetter *et al.* (2010) who concluded that adsorbed arsenate was oxidized based on XANES data shown in Figure 13.

Discussion

Without oxidation state data for adsorbed arsenic, it is difficult to draw conclusions from the experiments. It is interesting to note, however, that Amstaetter *et al.* did provide information on sorbed arsenic concentration. These results are provided in Table 6. A majority of the arsenic added to the reactors was adsorbed to goethite. Using XANES spectroscopy, they were able to show no oxidation of arsenite when exposed to goethite and no reduction of arsenate when exposed to goethite or Fe(II)/goethite systems. However, there was some evidence of oxidation of As(III) by the Fe(II)/goethite system.

Theoretical predictions of redox interactions between goethite and arsenic can be made by thermodynamic calculations. Standard redox potentials for goethite and arsenite are provided in Equations 15 and 16 below:

$$\alpha - FeOOH + 3H^+ + e^- \rightarrow Fe^{2+} + 2H_2O \qquad E^o = +0.335\,V \qquad \text{Eq. 15}$$

$$H_3AsO_3 + H_2O \rightarrow H_2AsO_4^- + 3H^+ + 2e^- \qquad E^o = -0.667\,V \qquad \text{Eq. 16}$$

To convert standard redox potentials to potentials reflecting the experimental conditions present, Equation 5 can be used. Equation 17 is the Nernst equation simplified

for a temperature of 298 K and converted from natural log to decadic log. Redox potentials can be generated for both iron and arsenic.

$$E = E^o - \frac{0.0591}{n} log \left(\frac{\Pi\ [reduced\ species]^m}{\Pi\ [oxidized\ species]^n} \right) \quad \text{Eq. 17}$$

To determine if a reaction is favorable, or will proceed spontaneously, the redox potentials of the reduced and oxidized species are compared. If Equation 18 results in a positive redox potential, the reaction is favorable.

$$E_{rxn} = E_{reduced} - E_{oxidized} \quad \text{Eq. 18}$$

As shown in Table 7, arsenite oxidation in the Fe(II)/goethite system is not predicted by thermodynamic calculations.

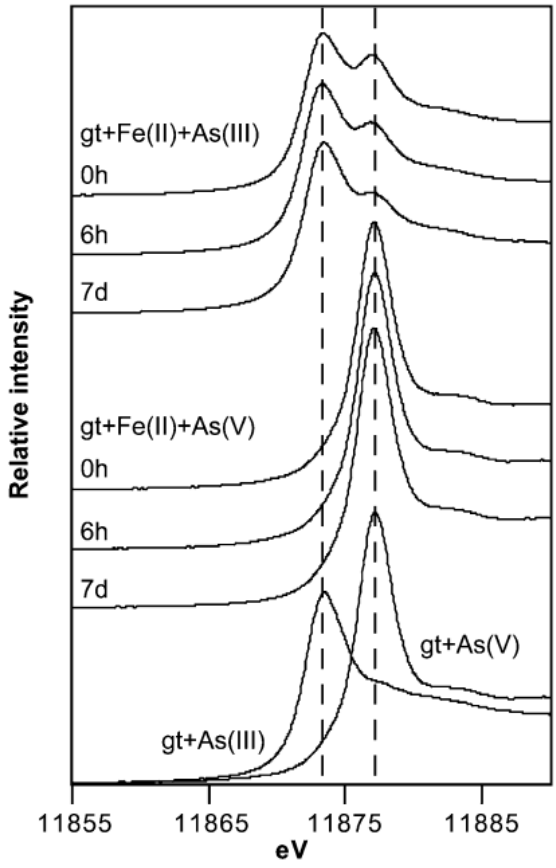

Figure 13. As-XANES Spectra Showing Arsenic Redox Transformation

(Amstaetter *et al.*, 2010)

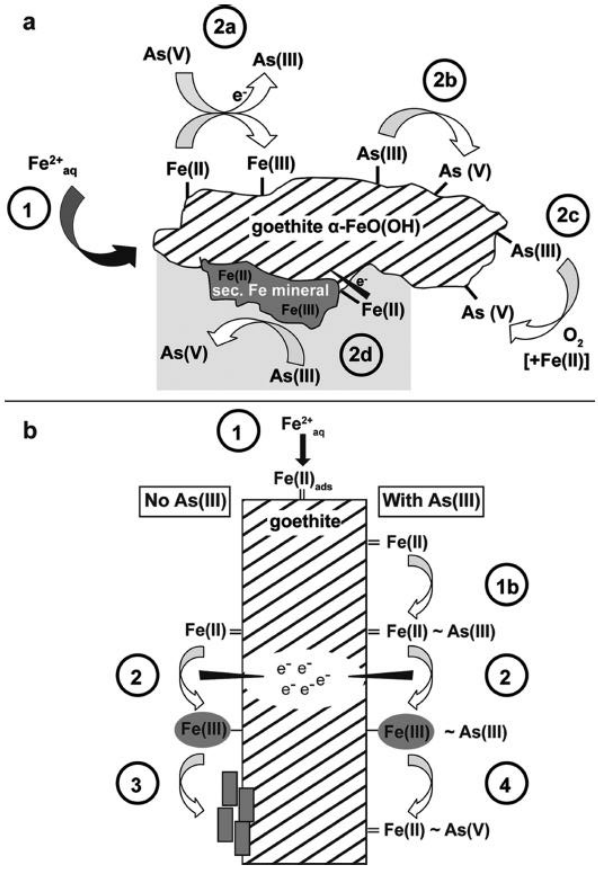

Figure 14. (a) Scheme Showing Possible Redox Reactions Between Fe(II), Goethite, and Arsenic. (b) Suggested Mechanism of Formation of Reactive Fe(III) Intermediate

(Amstaetter *et al.*, 2010)

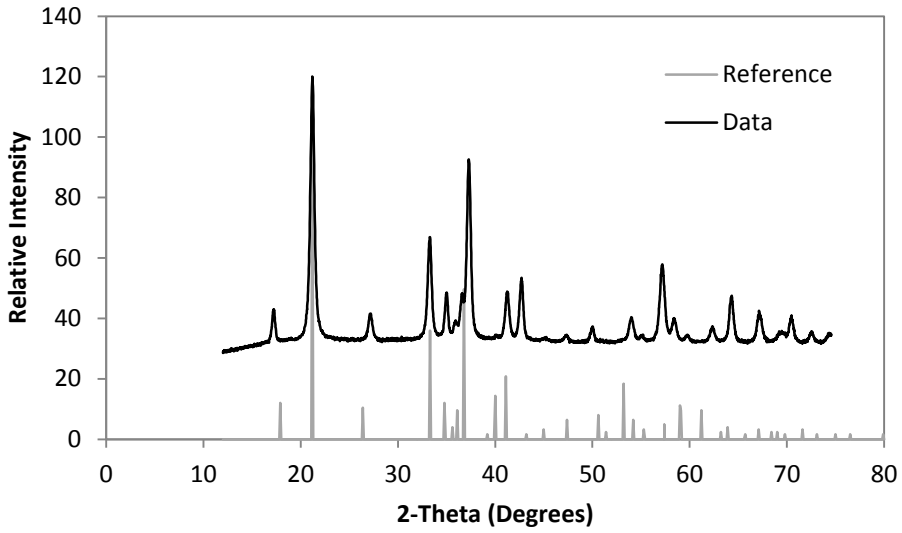

Figure 15. Goethite XRD Data Compared to Reference Spectrum

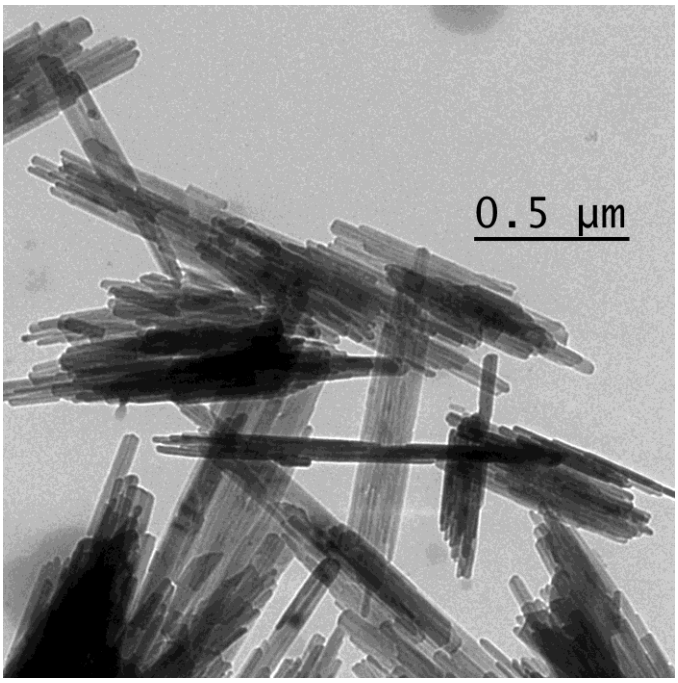

Figure 16. Micrograph of Goethite Rods

Table 5. Aqueous As Concentrations for As(III)/As(V) + Goethite Experiments

		As(III) (%)	**As(V) (%)**	**As(III) (µg/L)**	**As(V) (µg/L)**	**As in Solution (%)**
Gt+As(III)	Present Study	91	9	14	1*	1
	Amstaetter *et al.*	100	ND	69	ND	6
Gt+Fe(II)+As(III)	Present Study	85	15	125	22	12
	Amstaetter *et al.*	89	11	114	14	11
Gt+As(V)	Present Study	ND	ND	ND	ND	0
	Amstaetter *et al.*	ND	ND	ND	ND	0

Note: ND = not detectable

All experiments ran for 7 days

*BDL = below detection limit of 1.55 µg/L

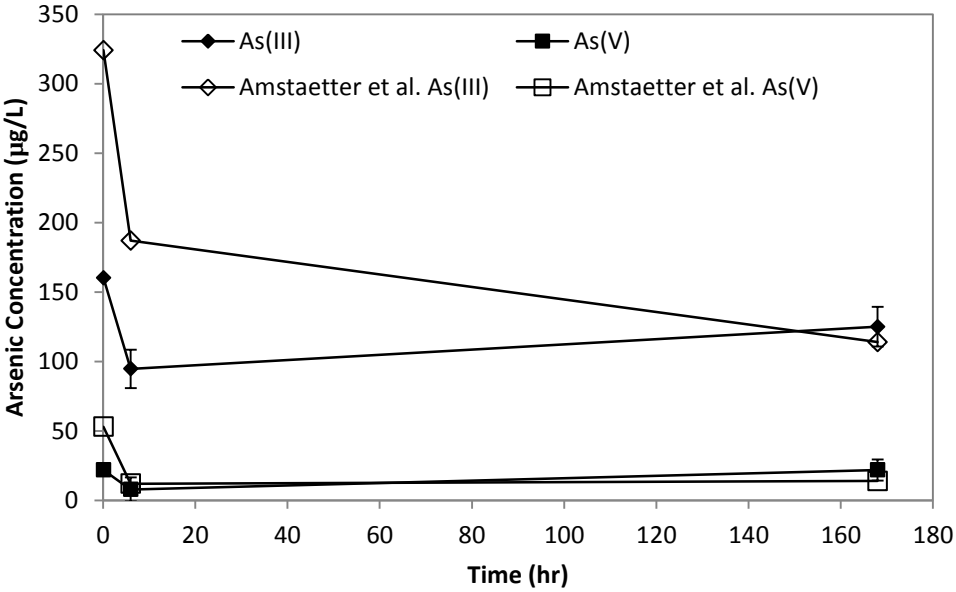

Figure 17. Aqueous As Concentration in Fe(II)/Goethite System

Error bars represent ±1 standard deviation

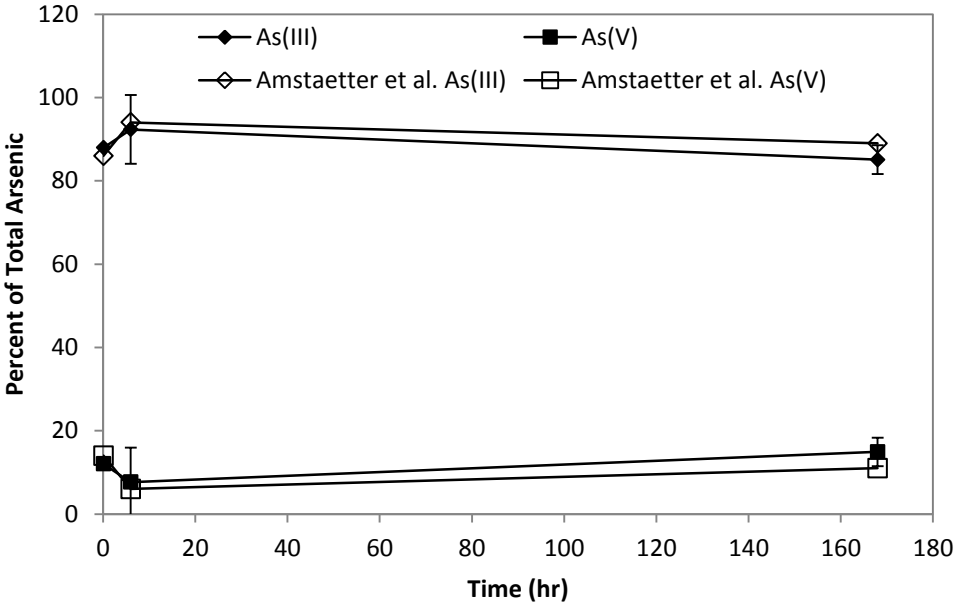

Figure 18. Percent Total Aqueous Arsenic in Fe(II)/Goethite System

Error bars represent ±1 standard deviation

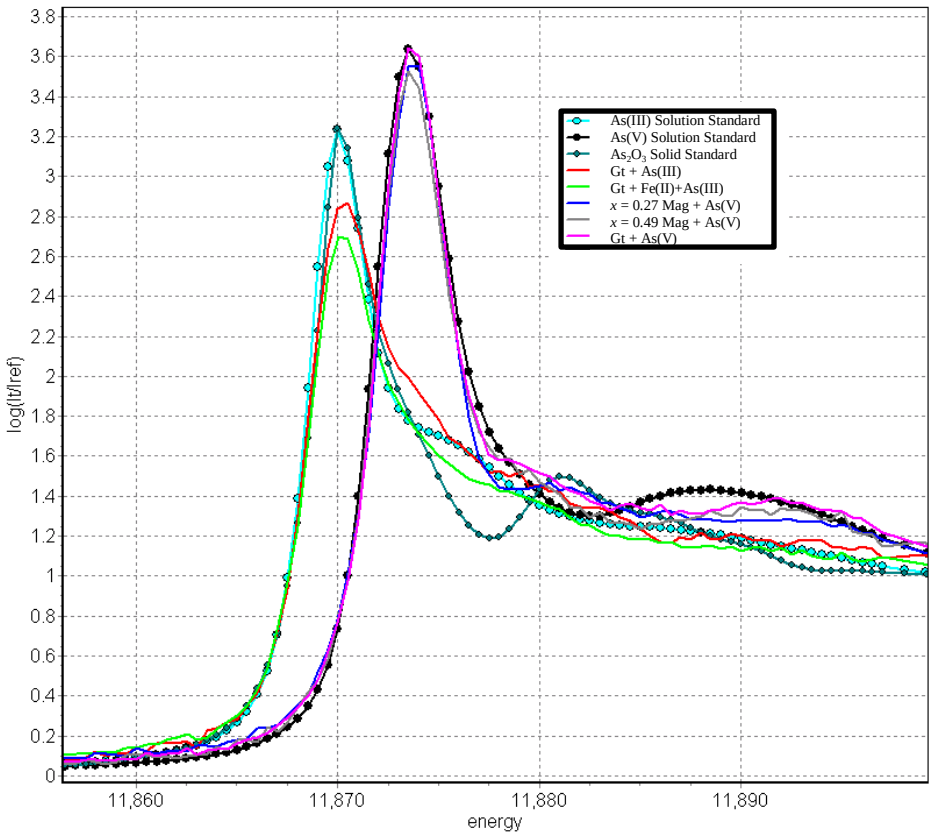

Figure 19. XAS Data for As and Iron Oxide Interactions

Note: Data provided by Max Boyanov at Argonne National Laboratory.

Table 6.Amstaetter et al. XANES Data for Adsorbed Arsenic

	Reaction Time	As(III) (%)	As(V) (%)	As(III) (ppm)	As(V) (ppm)	Sorbed As (%)
Gt+Fe(II)+As(III)	0 h	79	21	119	32	68
	6 h	84	16	154	29	82
	7 d	88	12	173	24	89
Gt+Fe(II)+As(V)	0 h	0	100	ND	221	99
	6 h	0	100	ND	221	99
	7 d	0	100	ND	221	99
Gt+As(III)	7 d	100	0	208	ND	94
Gt+As(V)	7 d	0	100	ND	221	99

Note: ND = not detectable

Table 7. Theoretical Redox Potential for Various Goethite/Arsenic Systems

	Reduced	**Oxidized**	**E_{rxn} (V)**	**Comments**
Gt+As(III)	goethite	As(III)	-0.501	$[Fe^{2+}] = 10^{-6}$ M, As(III):As(V) = 2000:1
Gt+As(V)	As(V)	Fe(II)	0.696	$[Fe^{2+}] = 10^{-6}$ M, As(III):As(V) = 1:2000
Gt+Fe(II)+As(III)	goethite	As(III)	-0.678	$[Fe^{2+}] = 10^{-3}$ M, As(III):As(V) = 2000:1
Gt+Fe(II)+As(V)	As(V)	Fe(II)	0.873	$[Fe^{2+}] = 10^{-3}$ M, As(III):As(V) = 1:2000

CHAPTER VI INTERACTIONS BETWEEN AS(V) AND MAGNETITE

Introduction

Magnetite is a mixed valent iron oxide. Magnetite stoichiometry, $x = Fe^{2+}/Fe^{3+}$, can range from $x = 0.5$ (stoichiometric) to $x = 0$ (completely oxidized), where the upper limit is set by the structure of magnetite. Fe(III) can exist in octahedral and tetrahedral sites, while Fe(II) only exists in octahedral sites of the magnetite structure. Magnetites with intermediate x values ($0 < x < 0.5$) are referred to as substoichiometric magnetites. The stoichiometry of magnetite has been shown to affect the rate of contaminant reduction (Gorski *et al.*, 2010). Figure 20 shows the effect of magnetite stoichiometry on the rate of nitrobenzene reduction (Gorski *et al.*, 2010). Figure 21 shows a linear trend between the natural log of the reduction rate of nitrobenzene and magnetite stoichiometry (Gorski *et al.*, 2010).

While magnetite has been proven to reduce many contaminants, no reduction of As(V) by magnetite has been shown. The research in this chapter was intended to show arsenate reduction. It was hypothesized that near-stoichiometric magnetite ($x = 0.49$) would reduce As(V) within the time frame of the experiment while substoichiometric magnetite ($x = 0.27$) would not.

Methods

Magnetite Synthesis

The magnetite synthesis method was adapted from two sources: Cornell and Schwertmann's The Iron Oxides: Structure, Properties, Reactions, Occurrence, and Uses

and the Regazzoni *et al.* (1981) article *Some Observations on the Composition and Morphology of Synthetic Magnetites Obtained by Different Routes*. In the glovebox, 250 mL 0.2 M $FeCl_3$ and 0.1 M $FeCl_2$ solutions were made and mixed together. 5 mL of 5 M HCl was added to the mixed solution to avoid ferric iron precipitation, whereupon the solution color changed from orange to yellow. The solution was then stirred and 10 M NaOH was added until the solution pH was above 10, which caused the solution to turn black. The solution was allowed to mix overnight. For substoichiometric magnetite (x = 0.27), H_2O_2 was added and the solution was allowed to mix for another day. This step was not followed for stoichiometric magnetite (x = 0.49). The solution was filtered and washed with DI water. The solids were then placed in a freeze dry vessel and taken out of the glovebox. The vessel was placed on the cooled freeze drier and the solids were given eight to twelve hours to dry. The vessel was then put back into the glovebox where the dried solids were dried and sieved through a 100 mesh sieve. Both magnetites (x = 0.27 and x = 0.49) were stored in the glovebox to prevent oxidation.

Magnetite Characterization

The specific surface area of magnetite can be measured on the BET as discussed in Chapter 3. Magnetite used in these experiments had specific surface area of approximately 60 m^2/g.

Powder x-ray diffraction (pXRD) with a cobalt source was used to verify the crystal structures of the prepared magnetite. Magnetite run on the pXRD was prepared with glycerol in the glovebox to prevent oxidation during analysis. No impurities were found in the synthesized magnetite using this method, however, a glycerol peak was

observed at $2\theta \approx 22^{o}$. Figure 22 shows the diffractogram produced by the low x magnetite sample along with magnetite's characteristic diffraction pattern.

Transmission electron microscopy (TEM) was used to image the magnetite particles. The synthesized magnetite particles were small and round, which is the typical magnetite structure. Micrographs can also be used for particle sizing. Particle length and width can be used to estimate specific surface area with a few assumptions regarding the three dimensional shape of the particle. A micrograph of the prepared magnetite sample is shown in Figure 23.

Mössbauer spectroscopy can be used to determine the oxidation state and structure of iron oxides and sorbed iron in solid samples. Mossbauer spectra can be used to determine the stoichiometry (x = Fe^{2+}/Fe^{3+}) of magnetite samples. This is done by estimating the relative areas under the Fe(II) and Fe(III) peaks.

Dissolution can also be used to determine the stoichiometry of magnetite samples. This was done by dissolving ~10 mg of magnetite in 1 mL 5 M HCl overnight. Then serial dilutions were performed on both Fe(II) and total Fe samples. Hydroxylamine was added to the total Fe samples and ammonium fluoride was added to the Fe(II) samples. The 1,10-phenanthroline method was then performed according to Shilt, 1969. Fe(II) and total Fe concentrations were measured, and Fe(III) concentration was calculated as follows:

$$[Fe(III)] = [Total\ Fe] - [Fe(II)] \qquad \text{Eq. 7}$$

Using the dissolution method, the stoichiometry of two magnetite stocks was determined. The high *x* magnetite sample had an $x_{dissolution}$ of 0.49, nearly stoichiometric. The low *x* magnetite had an $x_{dissolution}$ of 0.27, which is fairly oxidized.

Magnetite Suspension Preparation

Suspensions of $x = 0.27$ and $x = 0.49$ magnetite were made with a solid loading of 1.5 g/L. The suspension was allowed to mix for at least 24 hours before adjusting the pH to a value of 7 using 0.2 M NaOH. After the pH stabilized, which took approximately two days, aliquots were taken and arsenic spikes were added.

Reactor Set-up

All experiments were performed at room temperature in a glovebox. 60 mL reactor vials were wrapped in aluminum foil to prevent photochemical reactions and filled with 50 mL of magnetite suspension. An arsenic concentration of 2 mg/L was added to each reactor vial. All sample conditions were prepared in triplicates. Conditions tested included:

1. $x = 0.27$ Magnetite + As(V)
2. $x = 0.49$ Magnetite + As(V)

Sampling Method

Magnetite interactions with arsenate were allowed to proceed for twenty-four hours before sampling. Samples were first passed through a 0.45 μm nitrocellulose filter to remove solids. Half of the filtered solution was passed through an As(V)-selective

cartridge to remove As(V) as discussed previously. 4.5 mL of the cartridge and non-cartridge samples was placed into a plastic ICP-MS sample tube along with 1 mL 50 µg/L rhodium (added as an internal standard). All samples were stored at 4^{o}C in a refrigerator until analysis on the ICP-MS.

Aqueous iron concentration and composition was determined using the 1,10-phenanthroline method (Schilt, 1969). Sample absorbance was read on a UV-vis spectrophotometer at a wavelength of 510 nm.

Analysis Method

As discussed previously, the ICP-MS was used to determine aqueous arsenic concentration in all samples. The spectrophotometer was used to determine aqueous iron concentration using the 1,10-phenanthroline method. The X-ray absorption spectrometer (XAS) was used to analyze adsorbed arsenic concentration and speciation.

Results

At least 95% of the arsenic adsorbed to magnetite particles in both experiments. Some reduction of As(V) was observed in the x = 0.27 and x = 0.49 magnetite aqueous samples, but the concentration of As(III) measured in both cases was 1 µg/L. The As(III) concentration measured was well below the method detection limit and cannot be used as evidence for As(V) reduction. Results for the aqueous phase x = 0.27 magnetite + As(V) and x = 0.49 magnetite + As(V) experiments are shown in Table 8.

Solid samples, measured by the XAS, did not show any signs of As(V) reduction in the presence of either x = 0.27 or x = 0.49 magnetite. This is evidenced by the

comparing the As(V) peaks for the samples to that of the As(V) solution standard. In both cases, there is no reduction in peak intensity or peak shift from the As(V) electron binding energy to the As(III) electron binding energy. Correspondingly, there is no increase in As(III) peak intensity for the samples. Results for the solid phase As speciation can be seen in Figure 19 of Chapter III. Lack of reduction of As(V) by magnetite has been documented before, but for magnetite samples without specified stoichiometry (Su and Puls, 2008).

Discussion

Theoretical predictions of redox interactions between magnetite and arsenic can be made by thermodynamic calculations. Standard redox potentials for magnetite and arsenate are provided in Equations 19 and 20:

$$Fe_3O_4 + 8H^+ \rightarrow 3Fe^{3+} + 4H_2O + e^- \qquad E^o = -0.078\,V \qquad \text{Eq. 19}$$

$$H_3AsO_4 + 2H^+ + 2e^- \rightarrow HAsO_3 + 2H_2O \qquad E^o = +0.667\,V \qquad \text{Eq. 20}$$

To convert standard redox potentials to potentials reflecting the experimental conditions present, Equation 17 can be used. Redox potentials can be generated for both iron and arsenic.

$$E = E^o - \frac{0.0591}{n} log\left(\frac{\Pi\,[reduced\ species]^m}{\Pi\,[oxidized\ species]^n}\right) \qquad \text{Eq. 17}$$

To determine if a reaction is favorable, or will proceed spontaneously, the redox potentials of the reduced and oxidized species are compared. If Equation 18 results in a positive redox potential, the reaction is favorable.

$$E_{rxn} = E_{reduced} - E_{oxidized} \quad \text{Eq. 18}$$

As shown in Table 9, arsenate reduction favorable with both the x = 0.27 and x = 0.49 magnetite, and the more reduced magnetite provides a considerably more favorable reaction than the more oxidized magnetite.

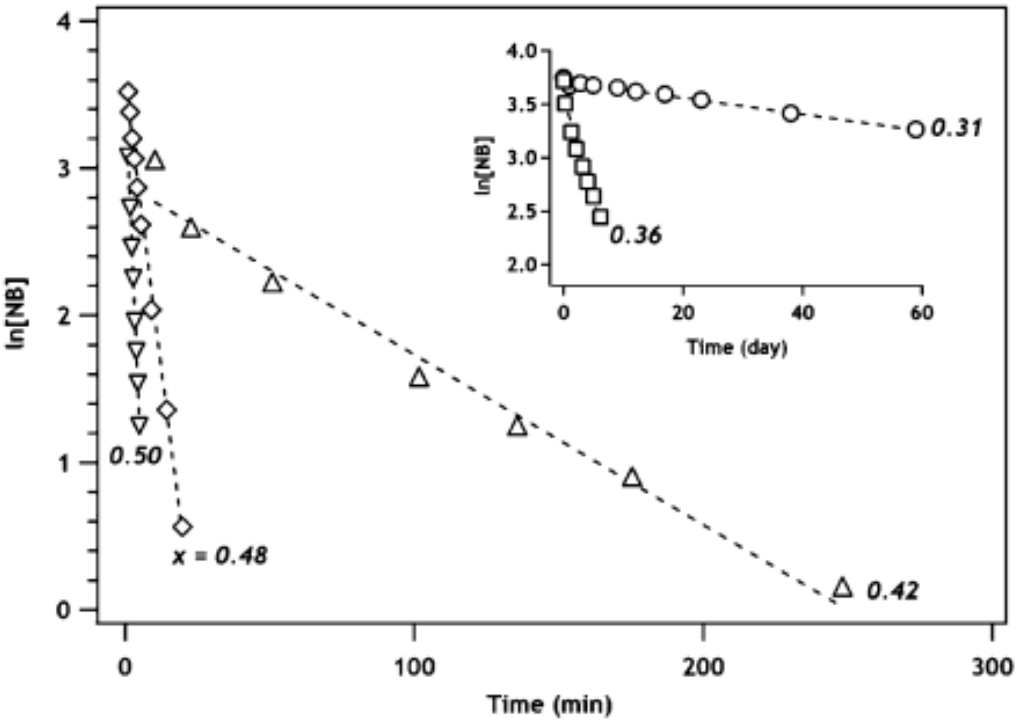

Figure 20. Effect of Magnetite Stoichiometry on Nitrobenzene Reduction Rate

(Gorski *et al.*, 2010)

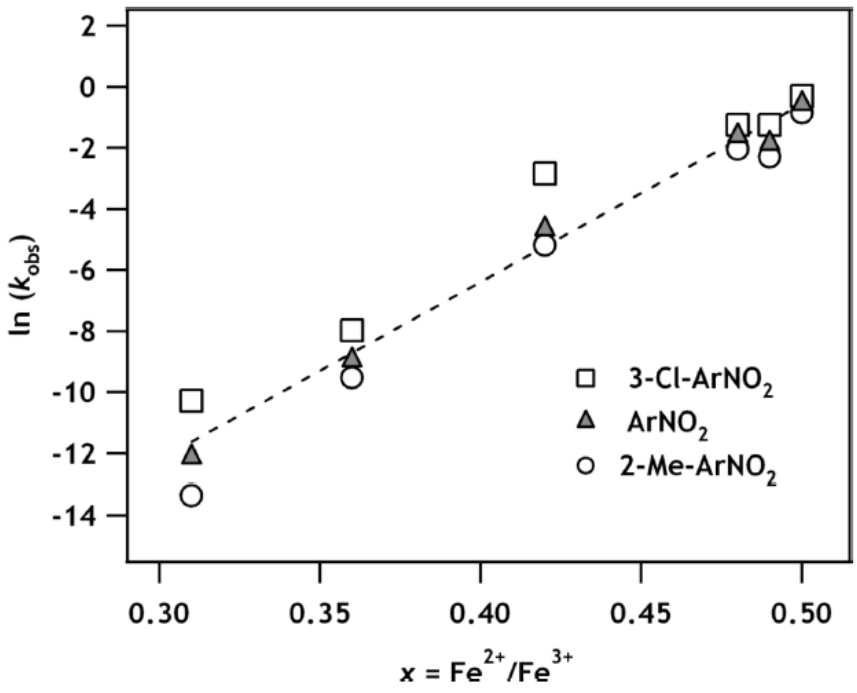

Figure 21. ln Nitrobenzene Reduction Rate vs. Magnetite Stoichiometry

(Gorski *et al.*, 2010)

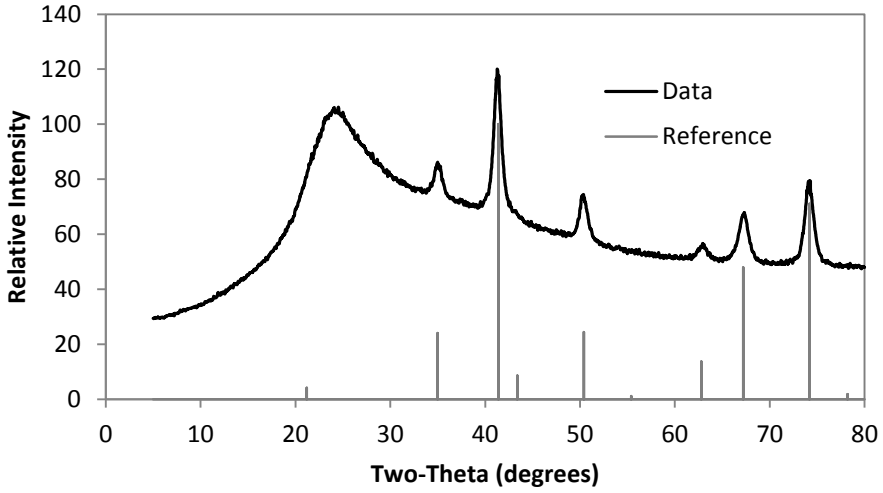

Figure 22. Magnetite XRD Data Compared to Reference Spectrum

Note: Peak intensity and width at 22^{o} enlarged due to glycerol.

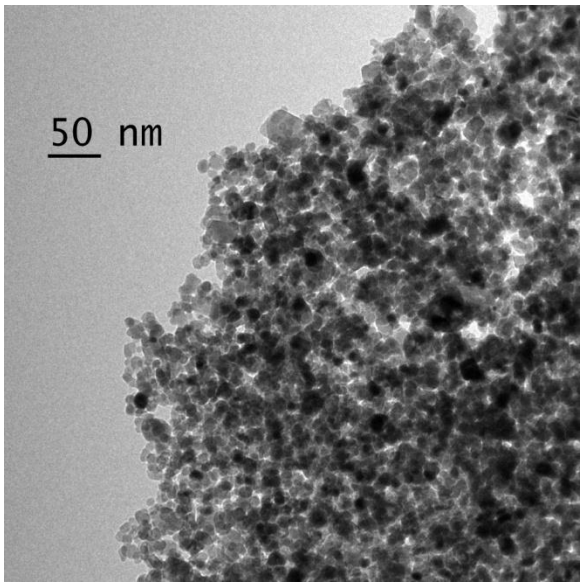

Figure 23. Micrograph of Magnetite Particles

Table 8. Aqueous As Concentrations for As(V) + Magnetite Experiments

	Reaction Time	**As(III) (%)**	**As(V) (%)**	**As(III) (µg/L)**	**As(V) (µg/L)**	**As in Solution (%)**
x=0.27 Mag+As(V)	1 d	1	99	1*	98	5
x=0.49 Mag+As(V)	1 d	100	0	1*	ND	0

Note: ND = not detectable

*BDL = below detection limit of 1.55 µg/L

Table 9. Theoretical Redox Potential for Various Magnetite/Arsenic Systems

	Reduced	Oxidized	E_{rxn} (V)	Comments
x=0.27 Mag+As(V)	As(V)	magnetite	0.434	$[Fe^{2+}] = 5 \cdot 10^{-6}$ M As(III):As(V) = 1:2000
x=0.49 Mag+As(V)	As(V)	magnetite	0.549	$[Fe^{2+}] = 10^{-4}$ M As(III):As(V) = 1:2000

CHAPTER V SUMMARY AND ENGINEERING SIGNIFICANCE

Summary of Results

This work has successfully applied an arsenic analysis method using ICP-MS and As(V)-selective cartridges. This method coupled with solid phase XAS analysis provided data regarding interactions between arsenic and Fe(II)/goethite and between arsenic and magnetite of different stoichiometries.

Oxidation of arsenite by the Fe(II)-goethite system was seen in the aqueous phase, which reflects the results presented in the Amstaetter *et al.* (2010) paper. There was not, however, any evidence of As(III) oxidation at the surface, which agrees with thermodynamic predictions but differs from the results shown by Amstaetter *et al.* (2010). Oxidation state changes were not seen in goethite suspensions spiked with either arsenite or arsenate.

Reduction of As(V) by magnetite was not shown to occur in either the high x or low x magnetite samples. Predictions were that arsenate reduction would occur in high x magnetite samples, but not in low x magnetite samples due to the difference in available Fe(II). Slow kinetics may account for the lack of arsenate reduction in high x magnetite samples.

Engineering Significance

The results provided by this research are significant despite the lack of observed redox activity. Thermodynamic calculations, as well as previous research (Gorski *et al.*, 2010), predict reduction of arsenate by magnetite. The fact that this does not occur is a

valuable addition to what we know about arsenic in the environment. Furthermore, as documented in this and other works (Mayo *et al.*, 2007), magnetite is a strong adsorbent of arsenic. The knowledge that magnetite will not reduce arsenate to arsenite, which would increase its mobility and toxicity, makes magnetite an even more attractive adsorbent for remediation of arsenic-contaminated sites.

There are significant differences between the results presented by Amstaetter *et al.* (2010) and the results of this work, which stresses the importance of reproducing experiments not just within the lab, but also at other research institutes. Based on this work, Fe(II)/goethite systems would not be suggested as an alternative for As(III) oxidation to the stronger adsorbate As(V).

Future Work

The work presented here provides a good foundation for many studies involving iron and arsenic. Past works have shown arsenic adsorption onto clays as well as As(III) oxidation (Lin and Puls, 2000). It would be interesting for future studies to investigate As(V) reduction by reduced clays. It is well known that dithionite is a strong reductant of clays (Stucki *et al.*, 1984). Once reduced, clays have been shown to be effective reducers of environmental contaminants including chromate (Taylor *et al.*, 2000) and uranyl (Chakraborty *et al.*, 2009). Recent work by our group has shown that Fe(II) is capable of reducing nontronite, an iron-bearing clay (Schaefer *et al.*, in press). The question of whether Fe(II)-reduced clay would reduce contaminants similarly to dithionite-reduced clays was subsequently posed. Arsenic studies would be an excellent way to investigate this question.

The non-intuitive result of As(III) oxidation by Fe(II)/goethite systems was not obtained in these experiments. Therefore, it would be interesting to look at Fe(II)/goethite + As(V) to see if the thermodynamically favorable reduction of arsenate takes place. Time permitting, longer time scales for redox experiments would also be beneficial to determine if these reaction occur very slowly or are simply not possible.

Furthermore, because aqueous arsenic concentrations are so small after reaction with iron oxides, it is critical to establish a low method detection limit to obtain a high degree of certainty in experimental results. For example, the goethite + As(III) results showed a small concentration of As(V) (1 µg/L) that, while below the detection limit of 1.55 µg/L, is too high to confidently claim that Fe(II) is the cause of As(III) oxidation in the Fe(II)/goethite + As(III) samples.

REFERENCES

Amonette, J. E. (2002). *Iron Redox Chemistry of Clays and Oxides: Environmental Implications.* Chantilly, VA: The Clay Minerals Society.

Amonette, J. E., Workman, D. J., Kennedy, D. W., Fruchter, J. S., & Gorby, Y. A. (2000). Dechlorination of Carbon Tetrachloride by Fe(II) Associated with Goethite. *Environmental Science and Technology*, 4606-4613.

Amstaetter, K., Borch, T., Larese-Casanova, P., & Kappler, A. (2010). Redox Transformation of Arsenic by Fe(II)-Activated Goethite (α-FeOOH). *Environmental Science and Technology*, 102-108.

Bard, A. J., Parsons, R., & Jordan, J. (1985). *Standard Potentials in Aqueous Solution.* New York: Marcel Dekker, Inc.

Bunker, G. (2010). *Introduction to XAFS: A Practical Guide to X-ray Absorption Fine Structure Spectroscopy.* New York: Cambridge University Press.

Carcinogen Assessment Group. (1980). *List of Carcinogens.* Washington, D.C.: Environmental Protection Agency.

Chakraborti, D., Rahman, M. M., Paul, K., Chowdhury, U. K., Sengupta, M. K., Lodh, D., et al. (2002). Arsenic Calamity in the Indian Subcontinent - What Lessons Have Been Learned? *Talant*, 3-22.

Chakraborty, S., Boivin, F. F., Gehin, A., Banerjee, D., Scheinost, A. C., Greneche, J. M., et al. (2009). Spectroscopic Investigations of Uranyl Reduction by Fe-bearing Clays. *Geochimica et Cosmochimica Acta*, A205-A205.

Charlet, L., S. E., & Liger, E. (1998). N-Compound Reduction and Actinide Immoblization in Surficial Fluids by Fe(II): The Surface Fe(III)OFe(II)OH Degrees Species, as Major Reductant. *Chemical Geology*, 85-93.

CHEEC. (2009). *Iowa Statewide Rural Well Water Survey Phase 2 (SWRL 2) Results and Analysis.* Iowa City, IA: The University of Iowa.

Cornell, R. M., & Schwertmann, U. (2003). *The Iron Oxides: Structure, Properties, Reactions, Occurrence, and Uses.* New York: VCH.

Cullen, W. R., & Reimer, K. J. (1989). Environmental Arsenic Chemistry. *Chemical Reviews*, 713-764.

Danielson, K. M., & Hayes, K. F. (2004). pH Dependence of Carbon Tetrachloride Reductive Dechlorination by Magnetite. *Environmental Science and Technology*, 4745-4752.

Dixit, S., & Hering, J. G. (2003). Comparison of Arsenic(V) and Arsenic(III) Sorption onto Iron Oxide Minerals: Implications for Arsenic Mobility. *Environmental Science and Technology*, 4182-4189.

Erickson, M. L., & Barnes, R. J. (2005). Glacial Sediment Causing Regional-Scale Elevated Arsenic in Drinking Water. *Ground Water*, 796-805.

Ficklin, W. H., & Callender, E. (1989). Arsenic Geochemistry of Rapidly Accumulating Sediments, Lake Oahe, South Dakota. *US Geological Survey Water Resources Investigation Report* (pp. 217-222). Phoenix: US Geological Survey Toxic Substances Hydrology Program.

Fredrickson, J. K., Zachara, J. M., Kennedy, D. W., Duff, M. C., Gorby, Y. A., Li, S. W., et al. (2000). Reduction of U(VI) in Goethite (a-FeOOH) Suspensions by a Dissimilatory Metal-reducing Bacterium. *Geochimica et Cosmochimica Acta*, 3085-3098.

Frost, R. R., & Griffin, R. A. (1977). Effect of pH on Adsorption of Arsenic and Selenium from Landfill Leachate by Clay Minerals. *Soil Science Society of America*, 53-57.

Fuller, C. C., Davis, J. A., & Waychunas, G. A. (1993). Surface Chemistry of Ferrihydrite: Part 2. Kinetics of Arsenate Adsorption and Coprecipitation. *Geochimica et Cosmochimica Acta*, 2271-2282.

Gao, Y., & Mucci, A. (2001). Acid Base Reactions, Phosphate and Arsenate Complexation, and their Competitive Adsorption at the Surface of Goethite in 0.7 M NaCl Solution. *Geochimica et Cosmochimica Acta*, 2361-2378.

Goldberg, S., & Glaubig, R. A. (1988). Anion Sorption on a Calcareous, Montmorillonitic Soil - Arsenic. *Soil Science Society of America*, 1297-1300.

Goldberg, S., & Johnston, C. T. (2001). Mechanisms of Arsenic Adsorption on Amorphous Oxides Evaluated Using Macroscopic Measurements, Vibrational Spectroscopy and Surface Complexation Modeling. *Journal of Colloid and Interface Science*, 204-216.

Gorski, C. A., & Scherer, M. M. (2009). Influence of Magnetite Stoichiometry on Fe(II) Uptake and Nitrobenzene Reduction. *Environmental Science and Technology*, 3675-3680.

Gorski, C. A., Nurmi, J. T., Tratnyek, P. G., Hofstetter, T. B., & Scherer, M. M. (2010). Redox Behavior of Magnetite: Implications for Contaminant Reduction. *Environmental Science and Technology*, 55-60.

Grimes, D. J., Ficklin, W. H., Meier, A. L., & McHugh, J. B. (1995). Anomalous Gold, Antimony, Arsenic, and Tungsten in Ground Water and Alluvium around Disseminated Gold Deposits along the Getchell Trend, Humboldt County, Nevada. *Journal of Geochemical Exploration*, 351-371.

Hansel, C. M., Benner, S. G., & Fendorf, S. (2005). Competing Fe(II)-Induced Mineralization Pathways of Ferrihydrite. *Environmental Science and Technology*, 7147-7153.

He, Y. T., & Hering, J. G. (2009). Enhancement of Arsenic(III) Sequestration by Manganese Oxides in the Presence of Iron (II). *Water, Air, and Soil Pollution*, 359-368.

Hindmarsh, J. T., & McCurdy, R. F. (1986). Clinical and Environmental Aspects of Arsenic Toxicity. *CRC Critical Reviews in Clinical Laboratory Sciences*, 315-347.

IARC. (2004). *Some Drinking-Water Disinfectants and Contaminants, Including Arsenic.* Lyon, France: WHO.

Klausen, J., Trober, S. P., Haderlein, S. B., & Schwarzenbach, R. P. (1995). Reduction of Substituted Nitrobenzenes by Fe(II) in Aqueous Mineral Suspensions. *Environmental Science and Technology*, 2396-2404.

Lin, Z., & Puls, R. W. (2000). Adsorption, Desorption and Oxidation of Arsenic Affected by Clay Minerals and Aging Process. *Environmental Geology*, 753-759.

Lovley, D. R., & Phillips, E. J. (1988). Novel Mode of Microbial Energy-Metabolism - Organic-Carbon Oxidation Coupled to Dissimilatory Reduction of Iron or Manganese. *Applied and Environmental Microbiology*, 1472-1480.

Mandal, B. K., Chowdhury, T., Samanta, G., Mukherjee, D. P., Chanda, C. R., Saha, K. C., et al. (1998). Impact of Safe Water for Drinking and Cooking on Five Arsenic-Affected Families for 2 Years in West Bengal, India. *The Science of the Total Environment*, 185-201.

Manning, B. A., Hunt, M. L., Amrhein, C., & Yarmoff, J. A. (2002). Arsenic(III) and Arsenic(V) Reactions with Zerovalent Iron Corrosion Products. *Environmental Science and Technology*, 5455-5461.

Mayo, J. T., Yavuz, C., Yean, S., Cong, L., Shipley, H., Yu, W., et al. (2007). The Effect of Nanocrystalline Magnetite Size on Arsenic Removal. *Science and Technology of Advanced Materials*, 71-75.

Meng, X., Korfiatis, G. P., Christodoulatos, C., & Bang, S. (2001). Treatment of Arsenic in Bangladesh Well Water using a Household Co-precipitation and Filtration System. *Water Research*, 2805-2810.

Mohan, D., & Pittman, Jr., C. U. (2007). Arsenic Removal from Water/Wastewater using Adsorbents - A Critical Review. *Journal of Hazardous Materials*, 1-53.

Mok, W., & Wai, C. M. (1990). Distribution and Mobilization of Arsenic and Antimony Species in the Coeur D'Alene River, Idaho. *Environmental Science and Technology*, 102-108.

Nakai, H., Miyano, Y., Hayashi, Y., & Isobe, K. (2006). Synthesis and Structural Characterization of a Photochromic Dirhodium Dithionite Complex: [((CpRh)-Rh-Ph)(2)(mu-CH2)(2)(mu-O2SSO2)](Cp-Ph=eta(5)-C5Me4Ph). *Molecular Crystals and Liquid Crystals*, 63-+.

National Research Council Subcommittee on Arsenic in Drinking Water. (1999). *Arsenic in Drinking Water.* Washington, DC: National Academy Press.

Nickson, R. T., McArthur, J. M., Ravenscroft, P., Burgess, W. G., & Ahmed, K. M. (2000). Mechanism of Arsenic Release to Groundwater, Bangladesh and West Bengal. *Applied Geochemistry*, 403-413.

Nordstrom, K. (2002). Worldwide Occurrences of Arsenic in Ground Water. *Science*, 2143-2145.

Ona-Nguema, G., Morin, G., Juillot, F., Calas, G., & Brown, Jr., G. E. (2005). EXAFS Analysis of Arsenite Adsorption onto Two-Line Ferrihydrite, Hematite, Goethite, and Lepidocrocite. *Environmental Science and Technology*, 9147-9155.

Ona-Nguema, G., Morin, G., Wang, Y., Foster, A. L., Juillot, F., Calas, G., et al. (2010). XANES Evidence for Rapid Arsenic(III) Oxidation at Magnetite and Ferrihydrite Surfaces by Dissolved O2 via Fe2+-Mediated Reactions. *Environmental Science and Technology*, 5416-5422.

Oremland, R. S., & Stolz, J. F. (2003). The Ecology of Arsenic. *Science*, 939-944.

Palmer, N. E., & von Wandruszka, R. (2010). Humic Acids as Reducing Agents: The Involvement of Quinoid Moieties in Arsenate Reduction. *Environmental Science and Pollution Research*, 1362-1370.

Peterson, M. L., White, A. F., Brown, G. E., & Parks, G. A. (1997). Surface Passivation of Magnetite by Reaction with Aqueous Cr(VI): XAFS and TEM Results. *Environmental Science and Technology*, 1573-1576.

Poulton, S. W., & Canfield, D. E. (2005). Development of a Sequential Extraction Procedure for Iron: Implications for Iron Partitioning in Continentally Derived Particulates. *Chemical Geology*, 209-221.

Rahman, M. M., Chowdhury, U. K., Mukherjee, S. C., Mondal, B. K., Paul, K., Lodh, D., et al. (2001). Chronic Arsenic Toxicity in Bangladesh and West Bengal, India - A Review and Commentary. *Journal of Toxicology-Clinical Toxicology*, 683-700.

Ramos, M. A., Yan, W., Koel, B. E., Zhang, W., & Li, X. (2009). Simultaneous Oxidation and Reduction of Arsenic by Zero-Valent Iron Nanoparticles: Understanding the Significance of the Core-Shell Structure. *Journal of Physical Chemistry C*, 14591-14594.

Regazzoni, A. E., Urrutia, G. A., Blesa, M. A., & Maroto, A. J. (1981). Some Observations on the Composition and Morphology of Synthetic Magnetites Obtained by Different Routes. *Journal of Inorganic and Nuclear Chemistry*, 1489-1493.

Reynolds, C. S., & Davies, P. S. (2001). Sources and Bioavailability of Phosphorus Fractions in Freshwaters: A British Perspective. *Biological Reviews*, 27-64.

Rochette, E. A., Bostick, B. C., Li, G., & Fendorf, S. (2000). Kinetics of Arsenate Reduction by Dissolved Sulfide. *Environmental Science and Technology*, 4714-4720.

Sadiq, M. (1997). Arsenic Chemistry in Soils: An Overview of Thermodynamic Predictions and Field Observations. *Water, Air, and Soil Pollution*, 117-136.

Schaefer, M. V., Gorski, C. A., & Scherer, M. M. (In Press). Spectroscopic Evidence for Interfacial Fe(II)-Fe(III) Electron Transfer in a Clay Mineral. *Environmental Science and Technology*.

Schilt, A. A. (1969). *Analytical Applications of 1,10-Phenanthroline and Related Compounds* (1st ed.). Oxford: Permagon Press.

Schwertmann, U., & Cornell, R. M. (2000). *Iron Oxides in the Laboratory: Preparation and Characterization* (2nd ed.). New York: Wiley-VCH.

Shilling, J. G., & Kingsley, R. (2001, July 30). *How Does it Work?* Retrieved May 1, 2010, from Welcome to the ICP-MS Laboratory: http://www.gso.uri.edu/icpms/

Smedley, P. L., & Kinniburgh, D. G. (2002). A Review of the Source, Behavior and Distribution of Arsenic in Natural Waters. *Applied Geochemistry*, 517-568.

Stratman, M., Bohnenkam, K., & J., E. H. (1983). An Electrochemical Study of Phase-Transitions in Rust Layers. *Corrosion Science*, 969-985.

Stucki, J. W., Golden, D. C., & Roth, C. B. (1984). Preparation and Handling of Dithionite-reduced Smectite Suspensions. *Clays and Clay Minerals*, 191-197.

Su, C., & Puls, R. W. (2008). Arsenate and Arsenite Sorption on Magnetite: Relations to Groundwater Arsenic Treatment Using Zerovalent Iron and Natural Attenuation. *Water Air and Soil Pollution*, 65-78.

Taylor, R. W., Shen, S. Y., Bleam, W. F., & Tu, S. I. (2000). Chromate Removal by Dithionite-reduced Clays: Evidence from Direct X-ray Adsorption Near Edge Spectroscopy (XANES) of Chromate Reduction at Clay Surfaces. *Clays and Clay Minerals*, 648-654.

Tongesayi, T., & Smart, R. B. (2007). Abiotic Reduction Mechanism of As(V) by Fulvic Acid in the Absence of Light and the Effect of Fe(III). *Water Research Commission*, 615-618.

UNICEF. (2008). *Arsenic Primer: Guidance for UNICEF Country Offices on the Investigation and Mitigation of Arsenic Contamination.* New York: UNICEF.

USEPA. (1999). *Analytical Methods Support Document for Arsenic in Drinking Water.* Washington, DC: USEPA.

Vikesland, P. J., Heathcock, A. M., Rebodos, R. L., & Makus, K. E. (2007). Particle Size and Aggreagation Effects on Magnetite Reactivity Toward Carbond Tetrachloride. *Environmental Science and Technology*, 5277-5283.

Voegelin, A., & Hug, S. J. (2003). Catalyzed Oxidation of Arsenic(III) by Hydrogen Peroxide on the Surface of Ferrihydrite: An In Situ ATR-FTIR Study. *Environmental Science and Technology*, 972-978.

Walker, M. M., Diebel, C. E., Haugh, C., Pankhurst, P. M., Montgomery, J. C., & Green, C. R. (1997). Structure and FUnction of the Vertebrate Magnetic Sense. *Nature*, 371-376.

Waychunas, G. A., Kim, C. S., & Banfield, J. F. (2005). Nanoparticulate Iron Oxide Minerals in Soils and Sediments: Unique Properties and Contaminant Scavenging Mechanisms. *Journal of Nanoparticle Research*, 409-433.

Webster, J. G., Nordstrom, D. K., & Smith, K. S. (1994). Transport and Natural Attenuation of Cu, Zn, As, and Fe in the Acid Mine Drainage of Leviathan and

Bryant Creeks. *Environmental Geochemistry of Sulphide Oxidation* (pp. 244-260). Washington, DC: American Chemical Society.

Welch, A. H., Westjohn, D. B., Helsel, D. R., & Wanty, R. B. (2000). Arsenic in Ground Water of the United States: Occurrence and Geochemistry. *Ground Water,* 589-604.

WHO. (1993). *Guidelines for Drinking-Water Quality, 2nd Edition.* Geneva: WHO.

Williams, A. G., & Scherer, M. M. (2004). Spectroscopic Evidence for Fe(II)-Fe(III) Electron Transfer at the Iron Oxide-Water Interface. *Environmental Science and Technology*, 4782-4790.

Wilson, F. H., & Hawkins, D. B. (1978). Arsenic in Streams, Stream Sediments and Ground Water, Fairbanks Area, Alaska. *Environmental Geology*, 195-202.

Yamamura, S. (2001). *Drinking Water Guidelines and Standards.* Geneva, Switzerland: WHO.

Zhang, H., & Selim, H. M. (2008). Competitive Sorption-Desoption Kinetics of Arsenate and Phosphate in Soils. *Soil Science,* 3-12.

APPENDIX A: EXTRACTION METHODS

Introduction

Before using XAS to determine arsenic oxidation state at the surface of the particles, extraction methods were attempted. Once arsenic is adsorbed onto iron oxide, it is strongly bound and difficult to extract from the solid. This point was proven with the attempt to extract arsenic from samples adding a high concentration of phosphate to samples in which arsenic had been given time to adsorb onto goethite, lepidocrocite, and maghemite; which resulted in arsenic recovery of 54%, 14%, and 1.6%, respectively (Manning *et al.*, 2002). Therefore, complete dissolution of iron oxide was deemed to be the best way to attain good arsenic recovery. Poulton and Canfield (2005) provided iron extraction procedures for both magnetite (using ammonium oxalate) and goethite (using sodium dithionite). Their methods provided near complete recovery of iron added to the systems (Table 1A), so it was chosen as the ideal method for arsenic extraction from the solid phase.

Ammonium Oxalate

After a 24 hour reaction period with As(V), magnetite solids were collected on nitrocellulose filters. Ammonium oxalate at pH 3.2 was used to dissolve magnetite collected on the filters. After the six hour dissolution time, the magnetite appeared to be fully dissolved. The sample was then run through a 0.45 μm filter, diluted, and tested for arsenic concentration and oxidation state, as described in Chapter II.

This method was successfully used to achieve a good mass balance for arsenic. Dissolution of magnetite by ammonium oxalate, however, could not be used to determine

oxidation state of arsenic at the time of sampling due to reduction of arsenate by ammonium oxalate. Results for arsenic speciation in samples containing As(V) and ammonium oxalate without magnetite can be seen in Table 2A.

Sodium Dithionite

Goethite solids were collected on nitrocellulose filters after reaction with arsenic. The solids were then dissolved in a pH 4.8 sodium dithionite solution for two hours. After dissolution, samples were filtered through a 0.45 μm filter, diluted, and tested for arsenic concentration and oxidation state as described in Chapter II.

This method was incapable of providing analyzable data because of interference of the internal standard, rhodium, by dithionite. Figure 2A shows a large reduction in rhodium counts for samples containing dithionite. A possible explanation for this is that dithionite formed a complex with rhodium (Nikai and Isobe, 2009), which reduced the amount of rhodium being ionized by the plasma and reaching the detector.

Conclusions

Extraction methods detailed by Poulton and Canfield (2005) could not be used for arsenic analysis in the present study. Ammonium oxalate, used to dissolve magnetite, caused As(V) to be reduced to As(III). Sodium dithionite, used to dissolve goethite, caused rhodium counts to plummet, possible due to the formation of a rhodium dithionite complex. Rhodium was used as an internal standard to standardize arsenic counts across samples, as discussed in Chapter II.

Table 1A. Efficiency of Phosphate at Extracting Arsenic

TABLE 1. Speciation of As(III) and As(V) in Solution and Phosphate Extracts of As(III)-Treated Fe^0, Rust-100 and Rust-40 Corrosion Products, and Iron Oxides

	solution			sorbed As_T	PO_4 extract		as recovery
material	(t = 0 h) $[As(III)]_0$ (%)	(t = 24 h) [As(III)] (%)	(t = 24 h) [As(V)] (%)	(t = 24 h) [As(III+V)] (%)	(t = 26 h) [As(III)] (%)	(t = 26 h) [As(V)] (%)	(t = 26 h) [As(III+V)] (%)
Fe^0-100	100[a]	ND[b]	11.7	88.3	ND	2.64	14.3
Fe^0-40	100	0.05	0.20	99.8	0.05	1.39	1.69
rust-100	100	37.1	0.76	62.2	5.49	6.13	49.5
rust-40	100	1.74	0.03	98.2	9.20	1.38	12.4
goethite	100	0.27	ND	99.7	53.9	ND	54.1
lepidocrocite	100	1.95	0.19	97.9	13.9	ND	16.1
maghemite	100	0.18	ND	99.8	1.63	ND	1.81
magnetite	100	100	ND				100
hematite	100	100	ND				100

[a] At t = 0, $[As(III)]_0$ = 0.20 mM, 1.000 ± 0.009 g solid in 25 mL. [b] ND = not detected.

Source: Manning, B. A., Hunt, M. L., Amrhein, C., & Yarmoff, J. A. (2002). Arsenic(III) and Arsenic(V) Reactions with Zerovalent Iron Corrosion Products. *Environmental Science and Technology*, 5455-5461.

Table 2A. Arsenic Oxidation State in As(V) + NH_4^+ Oxalate Samples

As Concentration (ug/L)	As(III) (cps)	As(V) (cps)	Tot As (cps)
1	2,631	-310	2,321
10	14,326	-797	13,529
100	109,007	22,630	131,637

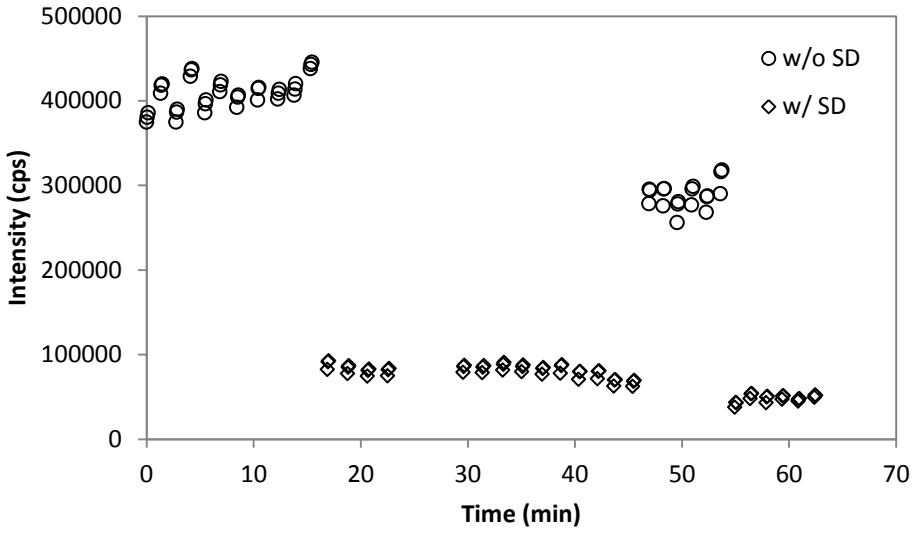

Figure 1A. Rhodium Count in Presence and Absence of Dithionite